PERGAMON

Deep-Sea Research II 48 (2001) 1733–1768

DEEP-SEA RESEARCH
PART II

www.elsevier.com/locate/dsr2

Configuring an ecosystem model using data from the Bermuda Atlantic Time Series (BATS)

Y.H. Spitz[a,*], J.R. Moisan[b,1], M.R. Abbott[a]

[a]*College of Oceanic and Atmospheric Sciences, Oregon State University, Corvallis, OR 97331-5503, USA*
[b]*Natural Science Division, Long Island University, New York, USA*

Abstract

The results of an assimilative approach to guide the configuration of an ecosystem model for the mixed layer of an oligotrophic environment are presented. The time series data from the US Joint Global Ocean Flux Study (JGOFS) Bermuda Atlantic Time Series (BATS), in conjunction with a data-assimilation scheme, were used to estimate the model parameters and modify the Fasham et al. (J. Mar. Res. 48 (1990) 591–639) (FDM) model. The evolution of the model from initial to final configuration was driven by: (a) the comparison of the time series data to the model results; (b) analysis of the estimated parameters; (c) observations of the BATS ecosystem from the literature; and (d) corrections of the model pathways. The data assimilation technique was crucial to estimate the optimal parameter set for each of the tested model configurations. The model presented in this paper includes several critical modifications to the FDM model. First, a variable chlorophyll-to-nitrogen ratio is introduced by solving a full equation for chlorophyll *a*. Second, zooplankton are split into two functional groups: nano/microzooplankton and mesozooplankton. Third, a new formulation is introduced for the microbial loop that is capable of resolving and simulating many of the processes observed in natural environments as well as in laboratory experiments, but had, until now, not been combined in a model. These modifications lead to solving an equation for the temporal evolution of the bio-active dissolved organic-carbon pool. This modified model, in conjunction with data assimilation, allowed us to estimate the model parameters and replicate the annual nitrogen cycle in the upper mixed layer at BATS. Bacteria were found to be a key player in controlling the size of the dissolved organic matter pool and in the amount of regenerated production.

* Corresponding author. Tel.: + 1-541-737-3227; fax: + 1-541-737-2064.
E-mail addresses: yvette@oce.orst.edu (Y.H. Spitz), jmoisan@osb.wff.nasa.gov (J.R. Moisan), mark@oce.orst (M.R. Abbott).
[1] Now at: NASA/66FC, Wallops Island, VA 23337, USA.

0967-0645/01/$ - see front matter
PII: S0967-0645(00)00159-4

1. Introduction

Biogeochemical models are increasingly being applied to a variety of regions in the ocean (Hofmann and Lascara, 1998). The original models from which most of the present models are adapted are small in number (e.g., Walsh and Dugdale, 1972; Wroblewski, 1977; Evans and Parslow, 1985; Frost, 1987; Fasham et al., 1990; Steele and Henderson, 1992). These models were first developed to simulate the annual nitrogen cycle in the upper ocean mixed layer and were later coupled to one-dimensional physical models (McGillicuddy et al., 1995a,b; Prunet et al., 1996a,b; Oguz et al., 1996; Doney et al., 1996) and embedded into three-dimensional circulation models (Fasham et al., 1993; Sarmiento et al., 1993; Moisan et al., 1996). The availability of observations from long term time series, such as Ocean Weather Station PAPA, Hydrostation "S", CalCOFI, two US JGOFS time series (Hawaii Ocean Time Series, HOT; Bermuda Atlantic Time Series, BATS), and process studies such as the North Atlantic Bloom Experiment (NABE) have allowed calibration of the various models. While these models can differ greatly in complexity and have been reasonably successful, they typically tend to either show poor agreement with the full set of observations or predict incorrect production rates.

Two main reasons for the inability of the models to simulate the observed biological-chemical fields are evident. First, all of these ecosystem models contain a large number of parameters whose values are poorly known. Some of these parameters (e.g., half-saturation coefficients, phytoplankton maximum growth rates) are determined either in situ or in controlled laboratory experiments. Other parameters (e.g., phytoplankton biomass-specific mortality coefficients) are difficult, if not impossible, to measure and are traditionally adjusted subjectively in the model until the "best" agreement between the simulation and the observations is reached. The values for these parameters may not be appropriate for ecosystems other than those to which they were tuned. Because of this, caution should be taken when using parameters that have been determined for an ecosystem from regions other than the one under study or taken from a different model. The task of determining the parameter set can become quickly tedious even for a simple model. Recently, data assimilation techniques, such as variational methods (Fasham and Evans, 1995; Lawson et al., 1996; Prunet et al., 1996a) and simulated annealing (Matear, 1995; Armstrong et al., 1995; Hurtt and Armstrong, 1996), have been applied to estimate the unknown parameters in the models.

While the estimation of the parameter set using the aforementioned techniques has led to an improvement in the model results, several studies have shown that the determination of the optimal set of parameters does not necessarily guarantee a good fit between the model results and the observations. This leads to the second reason for the difficulty in simulating ecosystem observations: inappropriate model structure and/or parameterization of the model pathways may be responsible for the misfit. For example, Fasham and Evans (1995), using the Fasham et al. (1990) (FDM) model, data from NABE, and an optimization technique to determine the optimal set of parameters, showed that it was impossible to reach a simultaneous good fit for the zooplankton biomass and primary productivity. Using a variational adjoint method and data from BATS, Spitz et al. (1998) demonstrated that the FDM model was unable to simulate adequately the seasonal cycle of the BATS ecosystem, and a set of optimal model parameters could not be estimated. Both studies concluded that further developments were needed to model the annual nitrogen cycle in the upper mixed layer. A first attempt to modify the FDM model for the BATS site was undertaken by Hurtt and Armstrong (1996), who simplified the FDM model and considered only four state

variables (nitrate, ammonium, phytoplankton, and a recycling compartment). They incorporated a variable nitrogen to chlorophyll ratio, modified the entrainment of nitrate at the base of the mixed layer, and took into account the effects of multiple size classes on phytoplankton growth and death rates and on export rates from the recycling compartment. They also used a regression model to fit the modeled concentrations to the data and to estimate the model parameters. Despite the improvement of the results, they showed that the assumptions made regarding ammonium concentrations are critically important to the quality of the fit to the available observations.

Our study is an attempt to use a data assimilation technique with observations from BATS not only to estimate the parameters of the model but also as a tool to modify the pathways in the ecosystem model while preserving model complexity such as explicit modeling of remineralization. The model used in this study is based upon the FDM mixed layer nitrogen budget model. This model has the advantage to predict quantities similar to the core measurements from the two US JGOFS long-term time series (SCOR, 1990). Furthermore, it was calibrated with the Hydrostation "S" observations between 1958 and 1960 Menzel and Ryther (1960), which provides us with a first guess parameter set for the assimilation procedure. Since the goal of the present study is to simulate the average annual cycle of the mixed layer biomass described by the BATS data, we utilized the climatological mixed layer in the assimilation process. This has the advantage that the model can be run forward in time to obtain a periodic solution that is not dependent upon the initial conditions of the model. On the other hand, this approach has the disadvantage in that it does not permit us to address the question of interannual variability of the ecosystem at BATS. A systematic analysis of the various terms within the model, the estimated parameters from the data assimilation, and the model results led to several modifications that improved the model results considerably and allowed for an estimate of the optimal set of model parameters. Only the final version of the model and the final model results are fully discussed in this paper.

The observations used during the assimilation process are described in Section 2. The data assimilation technique and the definition of the cost function are given in Section 3. The important modifications made to the original Fasham et al. (1990) model are presented in Section 4 and the model equations are presented in Appendices A and B. Results and discussion of the modified model using parameters determined during the assimilation process are in Section 5. Conclusions are given in Section 6.

2. Observations

The data used are the core measurements from the Bermuda Atlantic Time Series (BATS) station between 1988 and 1993 (Michaels and Knap, 1996). The observations are monthly measurements of nitrate, chlorophyll *a*, particulate organic nitrogen, and particulate organic carbon concentrations, bacteria cell counts, phytoplankton primary production, and bacterial production rates. Additional information on mesozooplankton biomass collected monthly during 1994–1996 (L. Madin, personal communication) are also added to the core measurement data set and used in the penalty cost function (see Section 3).

Since the model assumes that the ecosystem concentrations and processes are homogeneous within the mixed layer, the individual data profiles are vertically averaged from the surface to the depth of the mixed layer, which is computed from the monthly mean climatological data set

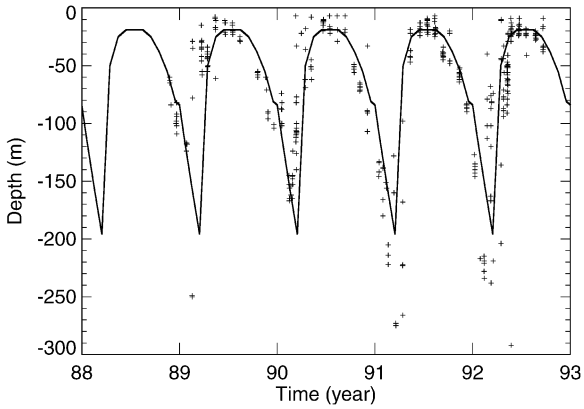

Fig. 1. The mixed layer depth (m), defined here as the depth at which the density is 0.02 kg m^{-3} lower than that observed at the surface. The solid line depicts the Levitus climatological mixed layer used in this study. The crosses designate the BATS data.

(Levitus, 1982). The depth of the mixed layer is defined as the depth where the density is 0.02 kg m^{-3} lower than that observed at the surface ($= 0.02$ kg m^{-3}). As a comparison, the mixed layer depths computed from the CTD data at BATS and the climatological data are plotted in Fig. 1. A strong deepening of the mixed layer occurs in winter to about 200 m, while the summer mixed layer shallows to about 20 m. The variability in the mixed layer depth is larger in winter than in summer due to decreased stratification and increased storm activity. The goal of this study is to simulate the average annual cycle of the mixed layer biomass described by the BATS data. Therefore, the effects of high frequency variability of the mixed layer depth, of spatial variabilities due to the passage of eddies (McGillicuddy et al., 1995a,b), and of interannual variations of the mixed layer depth (Doney, 1996) are considered as noise added to the monthly mean annual cycle of the ecosystem at BATS.

In order to compare model results and observations, ^{14}C primary production rates were converted to mmol N m^{-3} d^{-1} using a Redfield ratio of 6.625. The instantaneous growth rates from the model results were integrated over a full day so that they could be compared directly to the measured daily growth rates derived from the ^{14}C-uptake experiments.

Conversions were required for bacteria cell count data and bacterial production rates. Carlson et al. (1996) pointed out that there is no universally accepted conversion factor for converting bacterial abundance into carbon biomass or ^{3}H-TdR incorporation into bacterial carbon production. Furthermore, several studies (Sieracki et al., 1995; Carlson et al., 1996) show that 10–25% of the enumerated bacterial cells are prochlorophytes, not heterotrophic bacteria. Given the uncertainties in the conversion factors and measurements, bacteria biomass and production rates are not used in the assimilation process but rather taken as a reference of good fit. We assumed a constant bacterial carbon to nitrogen (C : N; mol:mol) ratio of 5 and a bacteria cell biomass of 20 fg C $cell^{-1}$ (Carlson et al., 1996) to calculate a conversion factor of 0.042 mmol N m^{-3} $(10^8$ cells $kg^{-1})^{-1}$ for bacteria cell count. The bacterial production rate was computed from ^{3}H-TdR incorporation experiments described in Carlson et al. (1996) and using the following formula:

$$BP = (TdR)ICF[biovolume]CCF\ CONV \quad (1)$$

where BP is the bacterial production (mmol N m^{-3} d^{-1}), TdR is the ^{3}H-TdR incorporation (pmol l^{-1} h^{-1}), ICF is the isotope conversion factor, CCF is the carbon conversion factor of 120 fg C m^{-3}, and CONV is the conversion factor from mg C l^{-1} h^{-1} to mmol N m^{-3} d^{-1}. The ICF was taken to be equal to 1.63 10^{18} cells mol^{-1} and the biovolume was set equal to 0.057 m^3 $cell^{-1}$. The observations are plotted in Fig. 5.

3. Optimization

The purpose of optimization is to find a set of parameters that minimizes the distance between the model estimates and the observations, i.e. the cost function. To achieve that goal, we used the variational adjoint method described in Lawson et al. (1995, 1996) and Spitz et al. (1998) with an optimization procedure based upon a limited memory quasi-Newton method (the N1QN3 subroutine from Gilbert and Lemaréchal (1989)).

The cost function (J) was defined in a least-squares manner as

$$J = \frac{1}{2} \quad (d_{,} - a_{,})^{\mathrm{T}} \mathbf{W} (d_{,} - a_{,}) + J_{\mathrm{p}}, \tag{2}$$

where d and a are the data and model equivalents to the data, respectively, i refers to the data types, and n refers to the observation time. J_{p} is a penalty function. The weighting matrices $\mathbf{W}$ are theoretically the inverse of the observation error covariance matrices. By assuming that errors in the data are uncorrelated and have equal variance, the weight matrices can be rewritten as

$$\mathbf{W} = w\,\mathbf{I}, \tag{3}$$

where w is a positive scalar and $\mathbf{I}$ is the identity matrix. In practice, w takes into account the relative magnitude of the various data types and the quality of the data sets. In this study, w accounts for the differences in the relative magnitude observed in the time average of each data type and is defined as

$$w = \frac{\max(d)}{d} \tag{4}$$

where d is the time average of the observation i, and $\max(d)$ is the maximum of the time average of the assimilated observations (Lawson et al., 1996). Since we wanted to keep the maximum degree of freedom on the parameters, no a priori information on the parameters was added to the cost function (Fasham and Evans, 1995; Matear, 1995). However, additional information on the nano/micro- and mesozooplankton biomass was added, and the penalty term J_{p} was defined such that the zooplankton biomass did not exceed the maximum value determined during two BATS cruises in August 1989 and March–April 1990 (Roman et al., 1993, 1995) and during the 1994–1996 mesozooplankton measurements (L. Madin, personal communication).

4. The ecosystem model

The model used in this study is based upon the FDM mixed layer nitrogen budget model. Following the results of assimilation experiments of the BATS data (Spitz et al., 1998) (Figs. 2a, b,

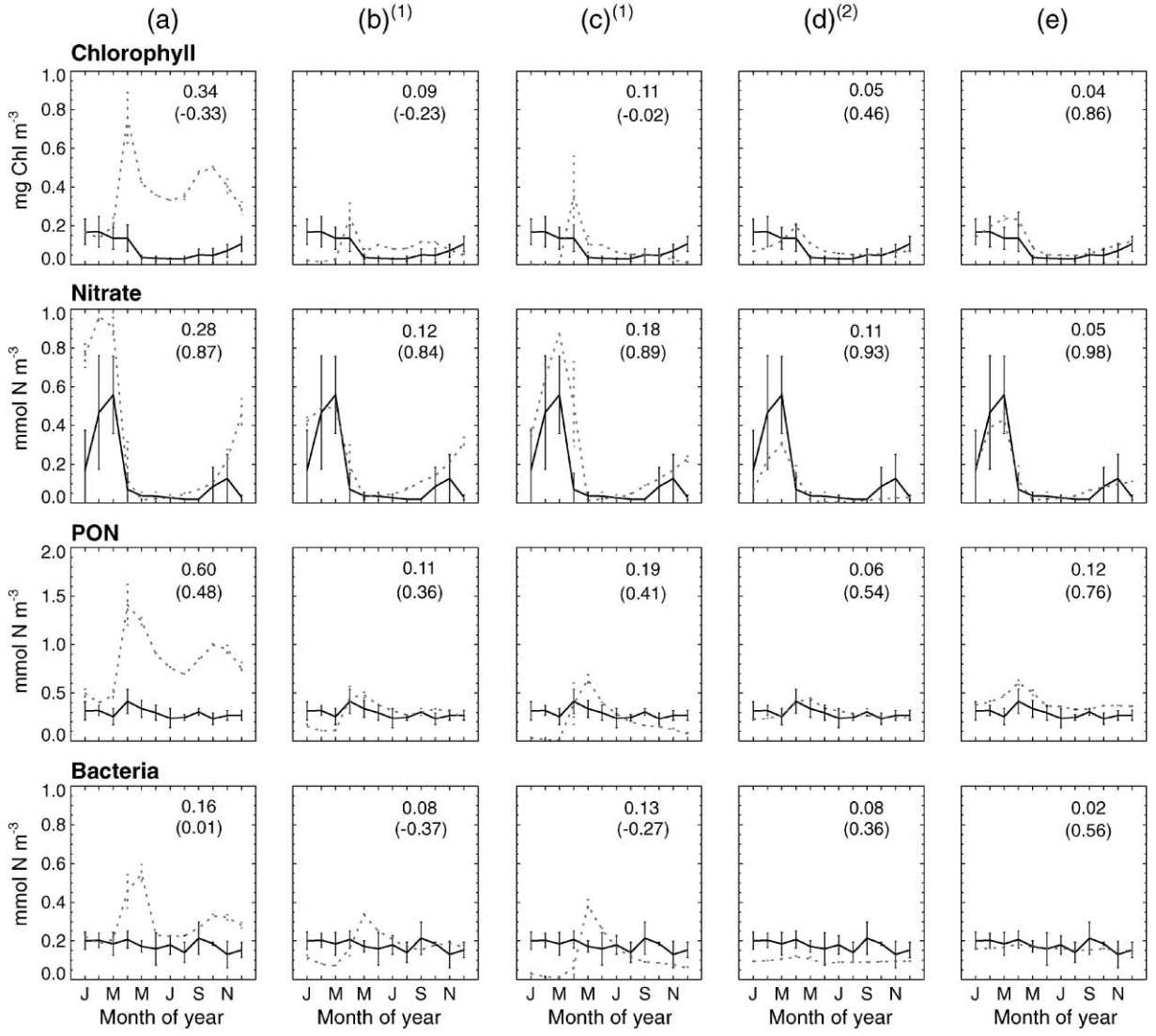

Fig. 2. Monthly mean and standard deviation of the observed chlorophyll *a*, nitrate, PON, bacteria at BATS (black solid line) and of the equivalent model results (red dashed line) over five years of simulation (1988–1993). The model results were taken at the same days as the BATS cruises. (a) represents the first guess run (Fasham et al. (1990) (FDM)), (b) corresponds to the results of the assimilation with the FDM model (Spitz et al., 1998), (c) represents the results of the assimilation with the modification of PAR and the nitrate input, (d) corresponds to the (c) case plus a temporal variable Chl*a*:N ratio, and (e) corresponds to the (d) case plus the modification of the microbial loop (new model). (1) indicates that some of the concentrations (not shown here) are out of the observed range for BATS. (2) indicates that some of the estimated parameters are out of range. The first number is the root-mean-square error (rms) (Eq. (C.1)), and the number in parenthesis is the correlation (*r*) (Eq. (C.2)).

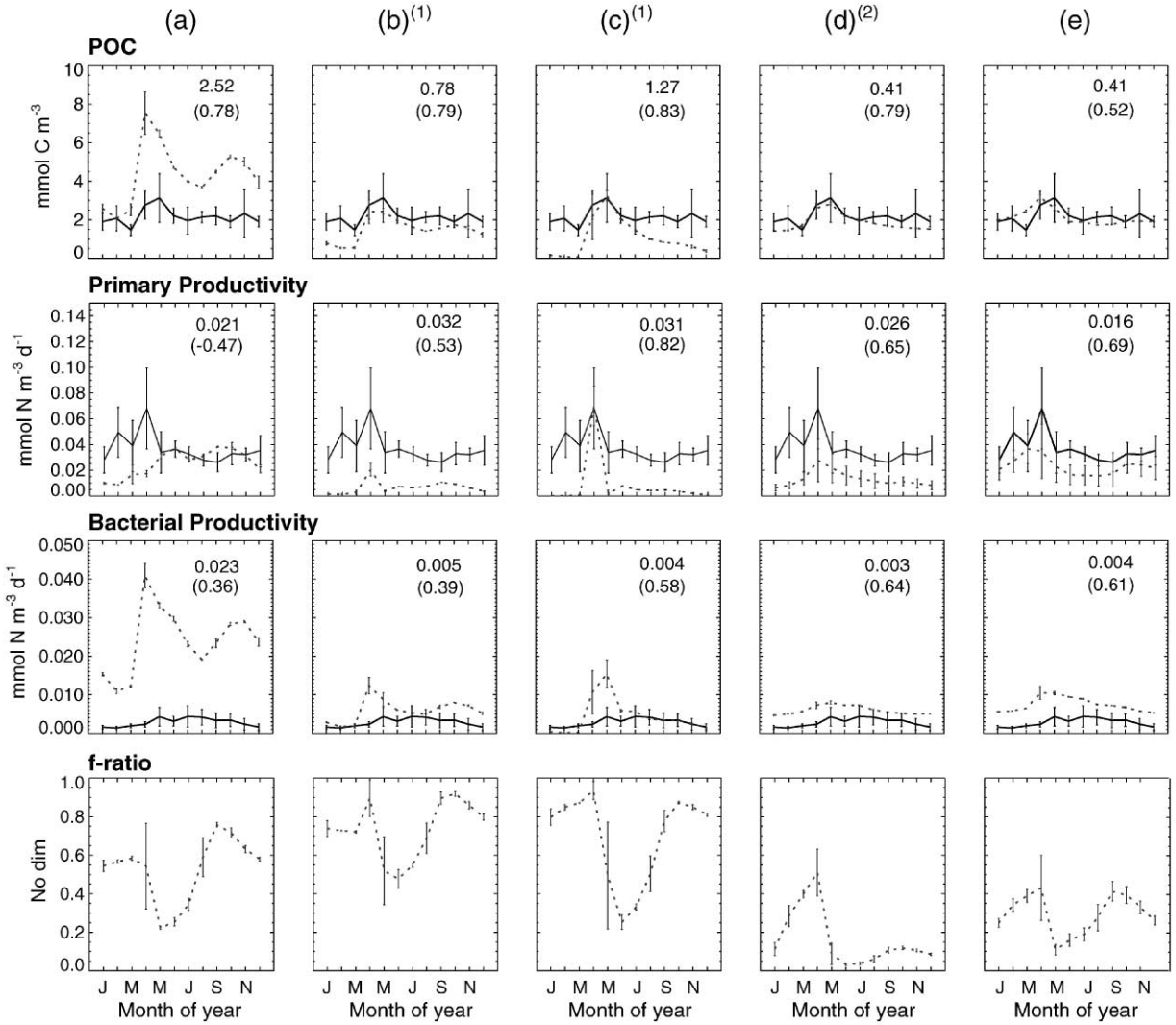

Fig. 3. Same as Fig. 2 but for POC, primary and bacterial productivity and *f*-ratio. The modeled *f*-ratio is plotted every day. POC concentrations were not modeled in cases (a)–(d), but computed as a sum of phytoplankton, zooplankton, bacteria and detritus with a C : N of 6.625 for phytoplankton and 5 for the other concentrations.

3a and b), it was clear that the ecosystem pathways needed to be modified to fit modeled and observed concentrations and rates. At every step of the modification process, a thorough analysis of the model results and the estimated parameters was undertaken. Once new problems were diagnosed, a survey of the literature was done to further modify the model. The full set of modified equations is given in Appendices A and B, the computation of root-mean-square error (rms) and correlation (r) are presented in Appendix C, and the steps taken during the assimilation procedure are described in Section 5. Following is a description of the primary modifications.

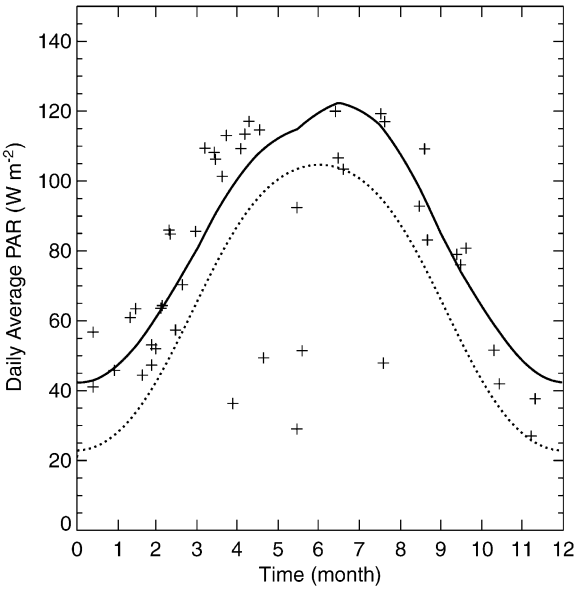

Fig. 4. Daily average Photosynthetically Available Radiation (PAR, W m^{-2}) just below the surface. The crosses are observed PAR at BATS from 1992 to 1994 (Siegel et al., 1995). The solid line corresponds to the values used in this study (see Appendix A). The dashed line corresponds to the values used in the FDM simulation.

4.1. Photosynthetically available radiation and nitrogen input

An identical twin experiment (Spitz et al., 1998) showed that the parameters involved in the model forcing terms were recovered first. This indicates that the light forcing and the nitrogen input into the mixed layer are important in controlling the ecosystem behavior. Photosynthetically Available Radiation (PAR) at the ocean surface is parameterized using classical astronomical formulae (Brock, 1981) and a model of cloud transmission (Evans and Parslow, 1985) with a cloud correction fitted to the Bishop and Rossow (1991) data set using the Moisan and Niiler (1998) model. This new approach gives a better fit between modeled and observed surface PAR (Siegel et al., 1995), especially during winter and fall (Fig. 4). In the FDM model, the nitrate concentration below the mixed layer is assumed constant over time and uniform with depth. The vertical profiles of nitrate at BATS show that the nitrate concentration is approximately constant to 100 m deep and then varies linearly with depth. The nitrate input formulation was then changed accordingly to match the observations at BATS (see Appendix A). These two modifications led to a better overall correlation between the modeled and observed concentrations but were not sufficient (Figs. 2c and 3c).

4.2. Chlorophyll-a-to-nitrogen ratio

Using data assimilation and a constant Chlorophyll-*a*-to-Nitrogen ratio (Chl*a*:N) [1.59 g Chl*a* (mol N)$^{-1}$], we were able to reduce the rms error between modeled and observed Chl*a* (Figs. 2b, c, 3b and c), but the correlation between the two time series remained poor. Higher

Chl*a* was constantly present in the April model results. We concluded that a temporally varying Chl*a*:N ratio is necessary in order to fit model results and observations. This is also in agreement with laboratory experiments (Laws and Bannister, 1980; Goldman, 1980; Geider, 1987, 1993; Kiefer, 1993) and in situ measurements (Campbell and Vaulot, 1993; Letelier et al., 1993) that have shown a wide range for the chlorophyll-carbon and chlorophyll-nitrogen ratios. Geider (1993) also showed that chlorophyll *a* accounts for a small and variable portion, 0.1–5%, of the phytoplankton organic matter, and it is therefore difficult to express chlorophyll *a* in terms of phytoplankton nitrogen. Despite the difficulties in determining the Chlorophyll-*a*-to-Carbon (Chl*a*:C) ratio, this ratio has been found to be highly regulated by light and nutrient availability, and temperature (Goldman, 1980; Geider, 1987, 1993; Cloern et al., 1995). Several modeling efforts (Doney et al., 1996; Hurtt and Armstrong, 1996) have adopted a variable Chl*a*:N ratio as a function of the irradiance and nutrient concentrations. In the modified model presented here, a temporally variable Chl*a*:C ratio is introduced by solving a phytoplankton chlorophyll equation (Appendix A) based upon the work of Geider et al. (1996, 1997). Modeled chlorophyll *a* is then fitted to observed chlorophyll *a*, and a constant C:N is estimated during the assimilation procedure.

4.3. Zooplankton species

In order to maintain a low zooplankton biomass and have adequate grazing of phytoplankton, it was necessary to split the zooplankton into two distinct functional groups, i.e. nano/microzooplankton and mesozooplankton. The nano/microzooplankton graze on bacteria, phytoplankton and detritus, while the mesozooplankton graze on phytoplankton and nano/microzooplankton. A constant C:N ratio is also estimated for the zooplankton.

4.4. Microbial loop

The results obtained with the previous modifications and assimilation are plotted in Figs. 2d and 3d. While the rms error decreased and the correlation increased, the results were still unsatisfactory. The modeled nano/microzooplankton concentration (not shown) was too large, and the modeled DON concentration (not shown) was found two orders of magnitude smaller than the observations in 1996. More importantly, some of the estimated parameters of the microbial loop were unrealistic. For example, zooplankton assimilation efficiency on bacteria was estimated to be equal to 113%. Modification of the microbial loop, reformulation of the flow pathways between the dissolved organic matter (DOM), bacteria and ammonium (NH_4, where the charge is ignored in future usage) pools, was found necessary.

Presently, oceanographers divide the DOM pool into labile, semi-labile and refractory pools. The refractory pool, by definition, has a very long turnover time. Deep water DOC has been aged using C-14 studies and has been found to be between 4000–6000 yr old (Druffel et al., 1992; Santschi et al., 1995). The semi-labile material has a turnover on scales of months to years, and the labile material turns over on scales of hours to days. Refractory DOM recently has been identified as being composed of a substantial amount of bacterial cell wall remnants (McCarthy et al., 1998). The semi-labile and labile pools are composed of nitrogeneous, carbohydrate and other Low Molecular Weight (LMW) materials. Because we are primarily interested in the seasonal cycling of organic matter, our model neglects the contribution that the refractory pool makes to the total

DOM pool. By assuming that the refractory DOM concentrations do not vary with depth and that the labile and semi-labile pools are only observed in the upper ocean (Carlson and Ducklow, 1995), it is possible to estimate the total amount of labile and semi-labile DOM observed at BATS by subtracting the observed concentrations of the deep-water DOM from the total DOM observed in the upper ocean. This allows us then to use the BATS DOM observations to compare against the model results.

Phytoplankton exudation or excretion is a major source of DOM. Several studies have shown that between 5 and 30% of the total marine phytoplankton primary production is released as DOM through exudation/excretion processes (Mague et al., 1980; Lancelot and Billen 1985; Baines and Pace, 1991). The various constituents in the phytoplankton exudates are carbohydrates, nitrogenous compounds, lipids and organic acids (Hellebust, 1974). The majority of this exudate is LMW DOM (Fogg, 1983). In a recent seawater culture experiment, Biddanda and Benner (1997) observed that phytoplankton exudate is composed of LMW DOM (65% of the DOM) with a C : N ratio of about 6 and High Molecular Weight (HMW) DOM with a C : N ratio of about 21. They also observed that rates of DOC production via exudation from phytoplankton ranged from 10 to 33% of the total organic carbon (TOC) production, and the carbohydrate fraction of the exudate was between 26 and 80% of the pool, increasing over the growth cycle. Because of these observations, we chose to divide the DOM pool into a carbohydrate and a nitrogenous DOM pool in our model.

Phytoplankton also have been shown to exude DOC in the form of carbohydrates during periods of nutrient limitation (Williams, 1990). This observation has given rise to a paradox in that the phytoplankton are supplying a carbon source to the bacteria at a time when the phytoplankton are nutrient limited and the bacteria are carbon limited. This supply of carbon to the bacteria stimulates bacterial growth and hence should increase the competition for the limiting nutrient (except during periods of silicate limitation). The observations of exudation of organic material by phytoplankton and its important role in DOM cycling convinced us to incorporate three distinct exudation terms in the model: a biomass-specific, a growth-specific and a nutrient-limitation exudation term. In the biomass-specific and growth-specific exudation terms, the exuded DOM material was assumed to have a C : N ratio close to that of the phytoplankton's cellular C : N ratio. The phytoplankton also were allowed to excrete excess carbohydrate during periods when the amount of sunlight energy being harvested was greater than that required for growth under the nutrient conditions present. This meant that during low-nutrient conditions, phytoplankton exuded a carbohydrate-type DOM.

Bacteria are the primary users of DOM. Heterotrophic bacteria can assimilate DON and NH_4, but they can also excrete NH_4 during DON catabolism (Kirchman et al., 1989). The assimilation or excretion of NH_4 by bacteria is very important in structuring the marine microbial loop. In the subarctic Pacific, the supply of dissolved free amino acids partially controls whether heterotrophic bacteria assimilate or excrete NH_4 (Kirchman et al., 1989). Based on the fact that a significant decrease in NH_4 uptake was observed when amino acids were added to the experiment, Kirchman et al. (1989) believed that in the subarctic Pacific, bacteria preferred to take up dissolved free amino acids over NH_4. When the amino acid supply was adequate, NH_4 was regenerated by bacterial assemblages that had been separated from the grazers. Furthermore, it was observed that the addition of carbohydrates reduces the potential for NH_4 regeneration and makes the bacteria a greater net sink for nitrogen. The uptake patterns of NH_4 and amino acids however seems to be

independent of the carbon source [glucose, acetate or citrate] used. High amino-acid recycling increases the availability of NH_4 to phytoplankton and potentially affects the plankton community structure (Kirchman et al., 1989). Concurrent uptake of NH_4 and amino acids also was observed in experiments by Goldman and Dennett (1991) and Kirchman et al. (1989). Experiments with amino acid additions into natural populations of bacteria observed concurrent uptake of NH_4 and amino acids only when a glucose source was present (Goldman and Dennett, 1991). Regeneration of NH_4 was evident only after the glucose source was completely utilized. NH_4 regeneration of actively growing bacteria seems to occur only under carbon-limiting conditions (Goldman and Dennett, 1991).

It is counterintuitive that the phytoplankton would release carbon-rich exudates during periods of nutrient limitation when laboratory results suggest that this will slow down nitrogen regeneration. However, measurable accumulations of DOM occur during the end of phytoplankton blooms. So, according to the above observations, NH_4 regeneration by bacteria is virtually stopped at the end of a bloom period, which further leads to the demise of the bloom by increasing the level of nutrient limitation.

Gross growth efficiencies of bacteria grown on various DOM substrates ranged from 94% when the C : N ratio of the substrate was low [1.5:1] and asymptotically reached a lower threshold value of 50% as the ratio increased above 3:1 (Goldman et al., 1987). The efficiency at which bacteria excreted NH_4 during amino acid catabolism was inversely related to the C : N ratio of the substrate. Under high C : N substrate ratios (10:1), there was virtually no NH_4 regeneration, while under low C : N substrate ratios (1.5:1) 90% was regenerated (Goldman et al., 1987).

Do bacteria prefer NH_4 over an amino acid substrate? It may be that the energetic costs of transportation of amino acids across the cell membranes may be high enough to offset the advantage of avoiding amino acid biosynthesis (Goldman and Dennett, 1991), resulting in no net gain between NH_4 uptake and amino acid uptake. If amino acids were the only source of nitrogen and carbon in marine waters, then not only would organic carbon control bacterial growth, but bacteria would play a major role in NH_4 recycling in the microbial loop (Goldman and Dennett, 1991).

Are the bacteria better scavengers of nitrogen than the phytoplankton? Some experimental evidence on the subject of bacteria/algal competition seems to suggest that this is true (Rhee, 1972; Parker et al., 1975; Parsons et al., 1981; Currie and Kalff, 1984a, b). This is theoretically expected considering the larger surface to volume ratio of the smaller bacteria (Bratbak and Thingstad, 1985). Bratbak and Thingstad (1985) found that in a chemostat situation where both heterotrophic bacteria and phytoplankton (*Skeletonema costatum*) were grown under conditions of low nutrients, the phytoplankton exudations supplied an additional source of phosphate to the bacteria that were then able to outcompete the phytoplankton.

This past decade, several efforts to model the microbial loop have been undertaken. FDM used DON as a proxy for DOC and assumed that during balanced growth conditions the ratio of uptake of DON and NH_4 should be constant in order to maintain a bacterial population with a constant C : N ratio. Remineralization of NH_4 was achieved only as a biomass specific respiration term. Anderson (1992) developed a general model that can be used for bacteria, copepods and microzooplankton. He considered two types of available substrates: one with only carbon and the other with carbon and nitrogen. In his model, the excretion of NH_4 was predicted based upon the C : N ratio of the substrates (DOM). Bissett et al. (1999) separated the DOM pool into a DOC, DON and

CDOC (colored DOC) pool. They allowed bacteria to remineralize the excess nitrogen taken up either as NH_4 or from the DON pool and to release it as NH_4. Vallino et al. (1996) separated the DOM pool into DON, DOC and refractory pools and used a bacterial bioenergetics model to investigate the utilization of DOM by bacteria.

The microbial loop that we developed in our model takes into account all of the recent observations outlined above. We assume that the bacteria are energy limited rather than nutrient limited. Given the large supply of DON in the ocean, its availability is only limited by the amount of energy that the bacteria can expend in acquiring this nutrient source. Because of this, the amount of available energy in the form of DOC that is available is first determined. This DOC source is obtained from both the carbohydrate-DOM and the nitrogenous-DOM supply. After accounting for the different gross growth efficiencies that are given to the two different energy forms, the amount of potential carbon left over for growth is calculated. This is then used to determine the amount of nitrogen required for growth. If more nitrogen is required than that obtained from the nitrogen taken up from the nitrogenous-DOM, then NH_4 uptake will be allowed. If more than the required nitrogen has been taken up, then the bacteria will be allowed to regenerate the excess nitrogen as NH_4. In this way, the bacteria are allowed to: (a) take up and regenerate NH_4; (b) have a variable gross growth efficiency that changes with the C : N ratio of the DOM substrate; and (c) alter the C : N ratio of the DOM pool by taking up the required C and N substrates as they become available. A complete derivation of the bacterial uptake is presented in Appendix B.

5. Results and discussion

At each step of the modification process, the model was solved using a fourth-order Runga–Kutta scheme with a 2-h time step. It was run first for 3 yr when it approached a steady annual cycle, and the data assimilation was done on the following 5 yr. This removed any effect that the initial conditions may have had on the recovery of the parameters. The initial guess for the parameter set (Table 1) was taken from FDM and values found in the literature, which allowed us to start the data assimilation procedure with a small misfit between the model results and the observations. After convergence of the assimilation procedure, the estimated parameters were used to run the direct model and generate the "fitted" time series shown in Figs. 2, 3 and 5.

In order to increase our confidence that the data assimilation solutions were not converging towards local minima of the cost function, the data assimilation process was restarted after perturbing the initial guess parameter values by first 20% and then 30%. All three model runs yielded the same set of parameters. Since some of the estimated parameter values were very close to their initial guess (Table 1), we verified that these parameters indeed could be estimated. A twin experiment was utilized for the verification process. The model output were considered as the data, and the initial guess for the model parameters was taken to be equal to the estimated values reduced by 40%. This experiment led to the recovery of all the parameters.

As seen in Figs. 2e and 3e, the fit between observations and modeled concentrations has been greatly improved when using the new model and data assimilation. In order to assess fully the success of the model with data assimilation in simulating the nitrogen cycle at BATS, it is necessary to analyze in detail the simulated fluxes as well as the estimated parameters. In fact, the resulting fluxes may be incorrect even though the modeled and observed concentrations agree, if the model

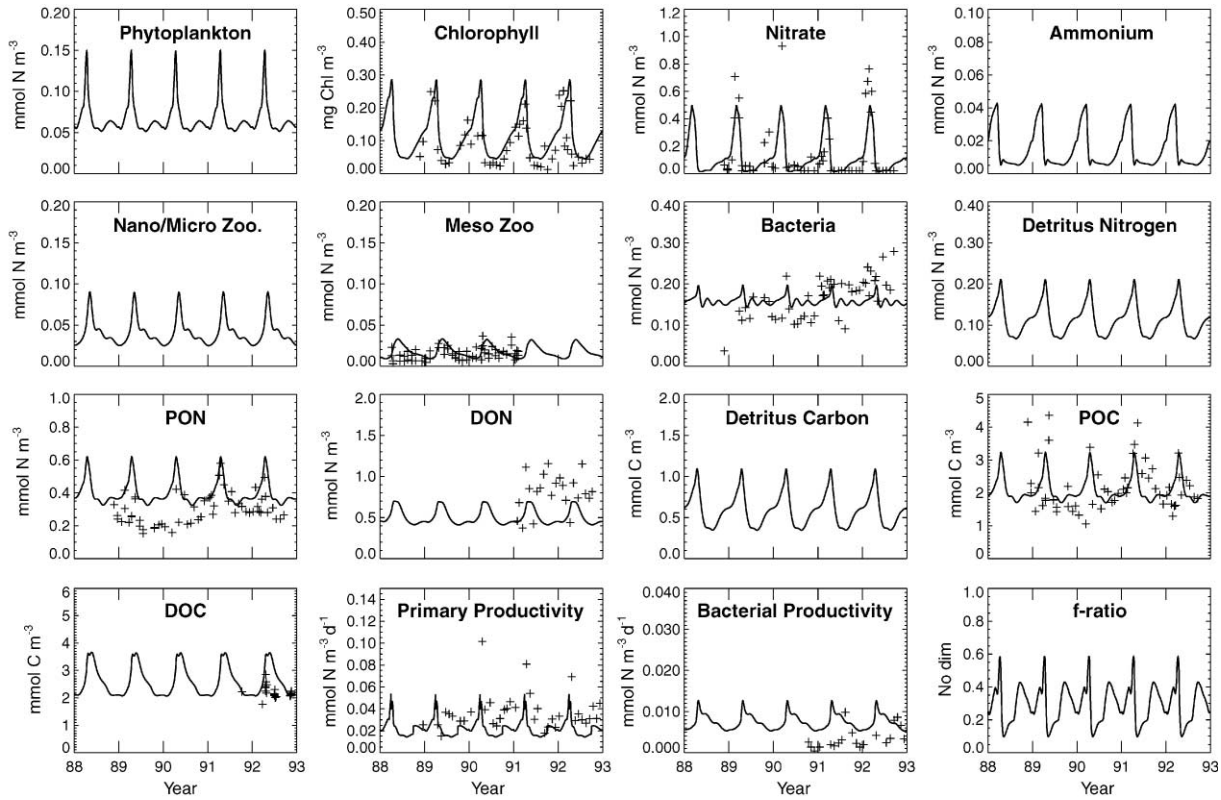

Fig. 5. Results of the new model with parameters estimated from the BATS data assimilation. The BATS data are represented by crosses. The mesozooplankton and the DOC observations are not available before 1994. The plotted mesozooplankton data are the day and night observations from 1994 to 1997 (L. Madin, personal communication). The depicted DOC observations correspond to the labile fraction of the DOC pool in 1994, according to Carlson and Ducklow (1996). The primary productivity observations have been corrected following Karl et al. (1998).

pathways are inaccurate. This analysis is often difficult since the information on fluxes and parameter values is sparse and often obtained during a limited number of cruises that might not be representative of a typical year. The assimilation results with the new model are discussed in the next three subsections.

5.1. Comparison of modeled concentrations with observations

The assimilated observations consisted of nitrate (NO_3^-, where the charge is ignored in future usage), chlorophyll *a*, particulate organic nitrogen, and particulate organic carbon concentrations. A good fit was obtained between both the simulated and observed chlorophyll *a* and NO_3 concentrations (Figs. 2e and 5). The largest misfit between simulated and observed NO_3 concentration occurs in spring when the mixed layer was the deepest and the climatological mixed layer was shallower than the observed 1988–93 mixed layer (Fig. 1). Consequently, the amount of modeled NO_3 entrained into the mixed layer during its deepening was less than the actual amount entrained

Table 1
Model parameters, initial guess values (IV) and estimated values (EV) using data assimilation

Parameter	Symbol	Unit	IV	EV
Pure seawater light attenuation coeff.	k	m^{-1}	0.04	
Chl *a*-specific light attenuation coeff.	k	m^{-1} (mg Chl *a*)$^{-1}$	0.03	0.028
Cross-thermocline mixing rate	m	m d^{-1}	0.1	0.11
Phyto. maximum growth rate	V_p	d^{-1}	2.9	3.67
Initial slope of the P/I curve		mg C (mg Chl *a* W m^{-2} d)$^{-1}$	1.0	1.23
Molecular weight of Carbon	MW_C	mg C (mmol C)$^{-1}$	12.0	
C : N ratio for phytoplankton	$C:N_P$	mmol C (mmol N)$^{-1}$	6.625	5.16
C : N ratio for bacteria	$C:N_B$	mmol C (mmol N)$^{-1}$	5.0	5.38
C : N ratio for nano/micro/mesozoo.	$C:N_Z$	mmol C (mmol N)$^{-1}$	4.0	5.02
C : N ratio for DOM-carbohydrate	$C:N_{DON}$	mmol C (mmol N)$^{-1}$	4.0	4.64
Maximum Chl *a* to C ratio		mg Chl *a* (mg C)$^{-1}$	0.08	0.041
Half-sat. for phyto. NO_3 uptake	K_1	mmol N m^{-3}	0.5	0.59
Half-sat. for phyto. NH_4 uptake	K_2	mmol N m^{-3}	0.1	0.04
Phyto. specific mortality rate	$_1$	d^{-1}	0.09	0.072
Phyto. biomass-specific exudation rate	$_1$	d^{-1}	0.05	0.066
Fract. of phyto. growth-specific exud.	$_2$	%	10	12
Fract. of phyto. nutrient-limitation exud.	$_3$	%	30	54
NH_4 inhibition parameter		(mmol N)$^{-1}$	1.5	1.48
Nano/microzoo. max. spec. grazing rate	g	d^{-1}	1.0	2.06
Nano/microzoo. assimilation efficiency	$_{1,\ 2,\ 3}$	%	70	61,87,45
Nano/microzoo. spec. excr./mort. rate	$_2$	d^{-1}	0.07	0.12
Fraction of nano/microzoo. growth-specific respiration		%	10	11
Nano/microzoo. half-sat. for ingestion	K_3	mmol N m^{-3}	1.0	1.2

Detrital fraction of nano/microzoo. mortality		%	15	18.9
NH_4 fraction of nano/microzoo. excretion		%	50	60.4
Nano/microzoo. food preference bact. rel. to phyto.	p_1	n.d.	1.0	1.14
Nano/microzoo. food preference det. rel. to bact.	p_2	n.d.	1.0	0.9
Mesozoo. maximum specific grazing rate	g	d^{-1}	1.0	0.78
Mesozoo. half-sat. for ingestion	K_5	mmol N m^{-3}	1.0	0.69
Mesozoo. assimilation efficiency	4, 5	%	70	72, 44
Mesozoo. spec. excr./mort. rate		d^{-1}	0.1	0.04
Fraction of mesozoo. growth-specific respiration	gl	%	10	11
Mesozoo. food preference nano/micro-zoo. rel to bact.	p_3	n.d.	1.0	0.95
Detrital fraction of mesozoo. mortality		%	15	15.15
NH_4 fraction of mesozoo. excretion		%	50	51.55
Bact. maximum growth rate on nitrogen	V_b	d^{-1}	1.0	0.25
Bact. specific respiration rate	3	d^{-1}	0.05	0.004
Bact. specific mortality rate	7	d^{-1}	0.01	0.0089
Bact. half-sat. for nitrogenous DOC uptake	K_{nitro}	mmol C m^{-3}	0.5	1.34
Bact. half-sat. for NH_4 uptake	K_{NH_4}	mmol C m^{-3}	0.5	1.01
Bact. half-sat. for carbohydrate DOC uptake	K_{carbo}	mmol C m^{-3}	0.5	1.33
Bact. gross growth efficiency of carbohydrate DOC	GGE_{carbo}	%	50	18.4
Bact. gross growth efficiency of nitrogenous DOC	GGE_{nitro}	%	50	62.8
Detrital breakdown rate	4	d^{-1}	0.025	0.031
Detritus specific breakdown rate by bacteria	6	(mmol N m^{-3})$^{-1}$ d^{-1}	0.025	0.026
Detritus sinking rate	V	m d^{-1}	1	1.35
Minimum NO_3 at $z < 100$ m	N_0	mmol N m^{-3}	0.2	0.39
Slope of the NO_3 for $z > 100$ m	N_{slope}	mmol N m^{-3} m^{-1}	0.02	0.03

into the mixed layer. For example, the observed maximum mixed layer depth in spring 1992 was 244 m while the climatological maximum depth was 196 m. The maximum modeled NO_3 concentration was 0.49 mmol N m^{-3} and the observed concentration was 0.76 mmol N m^{-3}. To assess the impact of the mixed layer depth on the NO_3 maximum, we ran the model with the same estimated parameter set and a maximum mixed layer of 244 m depth, the mixed-layer depth being the same for the rest of the year. We found that the maximum NO_3 concentration increased to 0.76 mmol N m^{-3}, which is equal to the measured value. As in Hurtt and Armstrong (1996), our model predicts a smaller seasonal variation in phytoplankton nitrogen than in chlorophyll *a*. The annual mean phytoplankton nitrogen is equal to 0.07 ± 0.02 mmol N m^{-3}, while the annual mean chlorophyll *a* is 0.11 ± 0.07 mg Chl m^{-3}. The Chl*a*:N ratio varies seasonally by a factor of three, which is similar to the range predicted by Hurtt and Armstrong (1996) and reported by Malone et al. (1993) for two cruises, August 1989 and March–April 1990.

The modeled particulate organic carbon (POC) and nitrogen (PON) concentrations also show good agreement with the observations (Figs. 2e, 3e and 5). The departure between modeled and observed PON/POC could be related to the working definition of PON. The modeled PON and POC concentrations were defined as the sum of contributions by phytoplankton, bacteria, nano/microzooplankton, mesozooplankton and detritus. By using 0.7 m GF/F filters, the measurements of PON and POC only represent particles larger than 0.7 m. Many bacteria are, however, smaller and therefore are not taken into account in the POM pool. Our model does not make any distinction in terms of sizes, and therefore small discrepancies are expected between measured and modeled PON/POC concentrations. The difference between the maximum modeled and observed concentrations of PON and POC also can be due to the fact that we use the climatological instead of the observed mixed-layer depth.

Despite the uncertainty in the conversion factor between bacteria cell counts and nitrogen biomass (mmol N m^{-3}), the modeled bacteria concentration is in the range of the measured concentrations using a conversion factor of 0.042 mmol N m^{-3} $(10^8$ cells $kg^{-1})^{-1}$ (Figs. 2e and 5). The detritus carbon concentration is lower than the values found by Roman et al. (1995) for the upper 100 m. They estimated a concentration equal to 1.97 ± 0.32 mmol C m^{-3} for the March–April 1990 ZOOSWAT cruises, while for dates corresponding to those cruises our model estimate is 0.86 ± 0.05 mmol C m^{-3}. This difference can be due to the fact that detritus is not directly measured but backcalculated from POC, bacteria, phytoplankton, nanozooplankton and microzooplankton biomass. Any measurement errors in one of these concentrations will result in errors in the detritus biomass. Furthermore, values used to convert microbial counts into C or N can have a large impact on the determination of detritus. Caron et al. (1995) showed that using low and high conversion factors for the microbial counts (see Table 1 from Caron et al., 1995) detritus nitrogen varies between 70 and 17% of total PON (0.38–0.09 mmol N m^{-3}) and detritus carbon varies between 75 and 31% of total POC (2.81–1.16 mmol C m^{-3}), respectively.

DOM observations are not part of the core measurements at BATS. Since 1994, TOC has been measured routinely, which allows us to compute the DOC concentrations as the difference between TOC and POC. Comparison between model results and observations however, is not straightforward. The DOC pool includes a labile, semi-labile and refractory part. From an experimental point of view, the refractory pool can be obtained from the deep values assuming that the refractory material is equally distributed throughout the water column (Carlson and Ducklow, 1995). Separating the semi-labile and labile pool is more difficult since the cycling

of the labile pool is very rapid. From unamended cultures exhibiting growth, Carlson and Ducklow (1996) reported that 6–7% of the bulk pool of DOC in the Sargasso Sea between 1992 and 1994 was a biologically labile fraction. This fraction would equal a biomass of ~ 2.9 to ~ 4.6 mmol C m^{-3} in 1994.

In our model, DOC represents the bio-active part of the DOC pool, and it was beyond the scope of this study to model separately the labile and semi-labile pools. The estimated turnover time varies between 0.18 and 1.59 days, with a minimum in early spring and a maximum in summer. The modeled DOC biomass (Fig. 5) varies between 2.1 and 3.7 mmol C m^{-3} with a maximum in early summer. The accumulation of ~ 2 mmol C m^{-3} after the spring bloom also has been observed at BATS (C. Carlson, personal communication). The molecular C : N ratio of the modeled DOM pool varies between 4.7 and 5.8, which would indicate that the DOM pool is mainly LMW DOM (Biddanda and Benner, 1997). Carlson et al. (1985) concluded that about 60% of the DOM pool in the surface ocean is LMW DOM. Furthermore, these low C : N ratios were observed by Biddanda and Benner (1997) in a culture of *Synechococcus* spp., the dominant phytoplankton species at BATS.

Since April 1994, L. Madin and co-workers (personal communication) have measured mesozooplankton biomass on a monthly basis. The data displayed in Fig. 5 were obtained from their night and day dry weight measurements when C = 0.4 dry weight and a C : N ratio of 5 were adopted to convert the observations to units of mmol N m^{-3}. Our model results show excellent agreement with these measurements. Recent observations of NH_4 (Lipschultz et al., 1996) reported lower values than during two ZOOSWAT cruises in August 1989 and March–April 1990 (Malone et al., 1993), mainly due to improved measurement techniques. According to Lipschultz et al. (1996), the mean NH_4 concentration for the mixed layer varies between a maximum of $\sim 5 \quad 10^{-2}$ mmol N m^{-3} after the spring bloom and a minimum of $\sim 5 \quad 10^{-3}$ mmol N m^{-3} in summer. These values are in excellent agreement with the modeled NH_4 concentrations, which vary between $5.2 \quad 10^{-3}$ and $4.26 \quad 10^{-2}$ mmol N m^{-3}. These values were reached despite the fact that we did not impose a priori information on the NH_4 concentration during the assimilation procedure, which was not the case in the assimilative work of Hurtt and Armstrong (1996).

5.2. Comparison of estimated parameters and rates with observations

The estimated parameters are reported in Table 1. The comparison between estimated and measured parameters is limited by the lack of measurements. Assimilating BATS observations between 1988 and 1993, Hurtt and Armstrong (1996) have estimated a half-saturation for nutrient uptake ranging from 0.0024 to 0.012 mmol N m^{-3}. The lowest value was obtained when a low NH_4 concentration constraint of 0.040 mmol N m^{-3} (Lipschultz et al., 1996) was imposed in the assimilation procedure, while the highest value was reached when the ZOOSWAT NH_4 measurements were assimilated. In our study, the half-saturation constants for NO_3 (K_1) and NH_4 (K_2) were found equal to 0.59 and 0.04 mmol N m^{-3}, respectively, while no NH_4 observations were assimilated. This difference between the values estimated by Hurtt and Armstrong (1996) and our estimates can be attributed to the difference in the nutrient uptake formulations used. Our estimated half-saturation constants for NO_3 and NH_4 uptake are in the range of values determined by Harrison et al. (1996) for the oligotrophic North Atlantic.

According to Malone et al. (1993), picoplankton accounted for 68% and 63% of the phytoplankton productivity during March–April 1990 and August 1989, respectively. The corresponding

percentages for the euphotic zone chlorophyll were 74 and 84%. This would indicate that *Synechococcus* spp. and prochlorophytes are dominant. A recent analysis of pigment composition from observations collected between 1990 and 1997 at BATS led to the same conclusion (D. Steinberg, personal communication). Our estimate of phytoplankton C : N ratio of 5.16 agrees with the C : N ratio found by Kana and Gilbert (1987) during growth experiments of *Synechococcus* spp. under various irradiances. They reported a C : N ratio equal to ~ 5.4 at a temperature of 22°C and PAR equal to 190 E m^{-2} s^{-1}, the yearly averaged mixed layer PAR at BATS.

From observations of growth rate and the Chl *a* : C ratio as functions of irradiance for laboratory cultures of various phytoplankton and using a least-squares fit model, Geider et al. (1997) were able to estimate the maximum Chl*a* : C ( ) and the initial slope of the P/I curve ( ). They found that in general cyanobacteria and dinoflagellates are characterized by low values of , and diatoms are characterized by high values. On the other hand, the highest values of were found for cyanobacteria. They found values between 0.015 and 0.072 mg Chl *a* (mg C)$^{-1}$ for and 0.55 to 9.63 mg (mg Chl *a* W m^{-2} d)$^{-1}$ for . Our estimates of and at BATS are in good agreement with the values found by Geider et al. (1997) for *Synechococcus* spp. Furthermore, the estimated (Chl*a* : C ratio) are in good agreement with the observations collected by Malone et al. (1993) during March–April 1990 and August 1989 cruises. Using their Chl*a* : C relationship integrated over the mean mixed layer depth for the two cruises, we estimated that $\ln(C/Chl) = 3.04 \pm 0.15$ in March–April and $\ln(C/Chl) = 4.34 \pm 0.09$ in August. From the model results corresponding to the dates of the two cruises, we found that $\ln(C/Chl) = 3.11 \pm 0.06$ in March–April and 4.24 ± 0.02 in August. Our estimate of phytoplankton maximum growth rate (V_p) is equal to 3.67 d^{-1}, which is in the range of values obtained considering the Eppley curve (Eppley, 1972). The temperature of the mixed layer at BATS typically varies between 21°C in winter and 28°C in summer, which leads to a maximum growth rate varying between 3.26 and 5.09 d^{-1}.

The maximum grazing (g) and excretion/mortality ($_2$) rates for nano/microzooplankton are found equal to about 3 times the respective rates for mesozooplankton (g and). This is consistent with the values determined by Hansen et al. (1997) for grazing rates as a function of the zooplankton body size. As expected, nano/microzooplankton preferentially graze on bacteria, then phytoplankton and detritus. Their assimilation efficiency is larger for bacteria than for phytoplankton and detritus.

The bacterial gross growth efficiency for carbon (GGE_{carbo}) was estimated by Carlson and Ducklow (1996) for BATS to be $14 \pm 6\%$. Our estimate of GGE_{carbo} (18.4%) is in that range. Our estimated biomass-specific growth rates for bacteria vary during the year from 0.04 to 0.07 per day, which is similar to the range 0.057–0.096 per day reported by Carlson et al. (1996). We are not aware of existing observations that can be directly compared with the other parameters of the microbial loop.

While the modeled primary productivity reproduces well the observed annual cycle and the late winter/early spring increase, it tends to underestimate the actual values. There are several possible causes. First, measurement errors can explain part of the discrepancy. The observations were integrated values over the climatological mixed layer of the mean light value (from three bottles) minus the dark value of the ^{14}C primary production rates. The mean error between the three replicates is on the order of 15%, with a maximum error of 57%. Secondly, the measured ^{14}C primary production rates were converted to mmol N m^{-3} d^{-1} using a constant Redfield ratio, which may introduce error. The third possible cause was pointed out by Karl et al. (1998)

who showed that by using GF/F filters, primary production can be overestimated by approximately 33%. In Figs. 3 and 5, we display the modified values (following Karl et al. (1998)) for primary productivity, and there is good agreement. Finally, a shallower climatological mixed layer depth than the observed depth can certainly explain the remaining small discrepancy between modeled and observed primary productivity in winter/early spring. In regards to the summer discrepancy, an alternative explanation would be that the summer production could be supported by other sources of new nitrogen such as nitrogen fixation.

The modeled bacterial production (BP) rates reproduce the temporal variation of the observations but, their values are higher than the observations (Figs. 3 and 5). Comparison between model results and observations is not easy in this case. Observed bacterial production rates were computed from ^{3}H-TdR incorporation rates that have shown high day-to-day variability in the upper 80 m (Carlson et al., 1996). Cell volumes used to estimate the BP rates also vary highly from day to day within each season. A single mean value for cell volume was used in Eq. (1), which could explain the shift between modeled and observed maximum BP rate.

The estimated *f*-ratio varies between 0.58 in winter and 0.09 in summer with an annual mean of 0.29. This estimate is consistent with the annual value of 0.31 derived by Platt and Harrison (1985) from NO_3 observations at Hydrostation "S" and results from other models (Doney et al., 1996; Hurtt and Armstrong, 1996).

5.3. Annual budget

Measuring annual fluxes within the marine ecosystem is difficult, if not impossible. Direct comparison between model results and observation is therefore not possible. We will only describe the modeled fluxes relative to each other and compare the results from several other model runs (Figs. 6–9). In the FDM simulation (Fig. 6), the parameter set was chosen such that the modeled annual net total production would fit that measured at Hydrostation "S" between 1958 and 1960. This simulation led to a large net annual upwards flux of NO_3. Phytoplankton loss by mortality was also very large, about 3 times larger than that due to grazing. Phytoplankton mortality was the largest source of detritus. The detrital breakdown to DON was about 71% larger than the detrital net downward flux. Bacteria took up DON in a larger amount than NH_4. Bacteria biomass-specific mortality was the main source of regeneration. The yearly net bacterial regeneration was 78% larger than the zooplankton regeneration.

In FDM simulation, the uptake of NO_3 by phytoplankton is 71% larger than the NH_4 uptake. However, considering that BATS and Hydrostation "S" are in an oligotrophic region, new production should be smaller than regenerated production ($f < 0.5$). Kinetics analysis (Harrison et al., 1996) also showed that NH_4 is preferentially utilized over NO_3 over the full range of NO_3 concentrations. Several studies (Williams, 1984; Biddanda and Benner, 1997) have postulated that 5–50% of the organic matter synthesized by phytoplankton is released as DOM. In the FDM simulation, this is of the order of 5%, which is at the low end of the observed range of values. Using FDM and data assimilation of the BATS data between 1988 and 1993 (Fig 7), the net upwards flux of NO_3, phytoplankton mortality, detrital breakdown to DON, and bacteria NH_4 excretion are largely reduced. However, the aforementioned problems still remain.

The mean annual fluxes obtained with the new model in conjunction with assimilation of the BATS data are plotted in Fig. 8. As in the previous run, the fluxes not related to the microbial loop

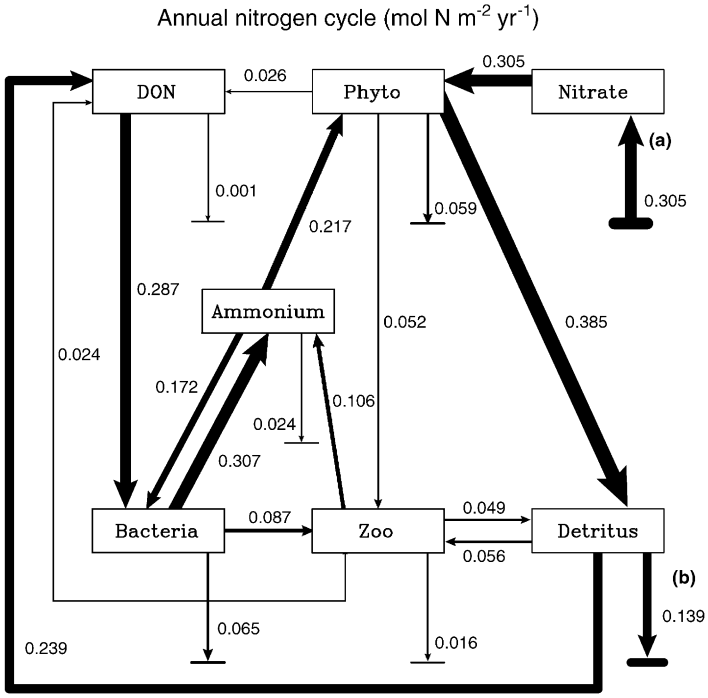

Fig. 6. Annual nitrogen cycle in mol N m^{-2} yr^{-1} obtained with the FDM model and their parameter set. (a) depicts the net nitrate upward flux (entrainment + diffusion), and (b) the net detritus downward flux (volumetric dilution + sinking + diffusion). The thickness of the line is proportional to the magnitude of the flux.

are largely reduced. The net upward flux of NO_3 in the mixed layer is about half of that estimated by FDM, which results in about half of the mixed layer new production. Using a variety of geochemical techniques that average over timescales of years to decades, the mean annual new production estimates for the Sargasso Sea range from 0.4 to 0.7 mol N m^{-2} yr^{-1} (Jenkins and Goldman, 1985; Jenkins, 1988; Spitzer and Jenkins, 1989). These estimates as well as the FDM results were largely constrained by data collected in the 1960*s*, a decade of deep mixing and strong blooms, while our modeled results were constrained by observations when the mixing was less extreme (Michaels et al., 1994). The uptake of NO_3 by phytoplankton is about half of the uptake of NH_4, which is consistent with the inhibition of NO_3 uptake by NH_4 observed by Wheeler and Kokkinakis (1990) and Harrison et al. (1996). The phytoplankton exudation of DOM is about 47% of the total production, which is consistent with the value found in the literature. The uptake of NH_4 by bacteria is about 10 times smaller than in the FDM simulation (not shown). However, the sum of the net regeneration by bacteria and bacteria biomass-specific excretion is of the same order of magnitude as the net regeneration in FDM. The yearly net bacterial regeneration is 66% larger than the zooplankton, compared to 78% in the FDM simulation. The zooplankton respiration is reduced about 30% compared to the value estimated in FDM.

In our simulation, the bacteria do not seem to compete with phytoplankton for NH_4, which was not the case in FDM. The bacteria uptake of NH_4 (note that only net regeneration of NH_4

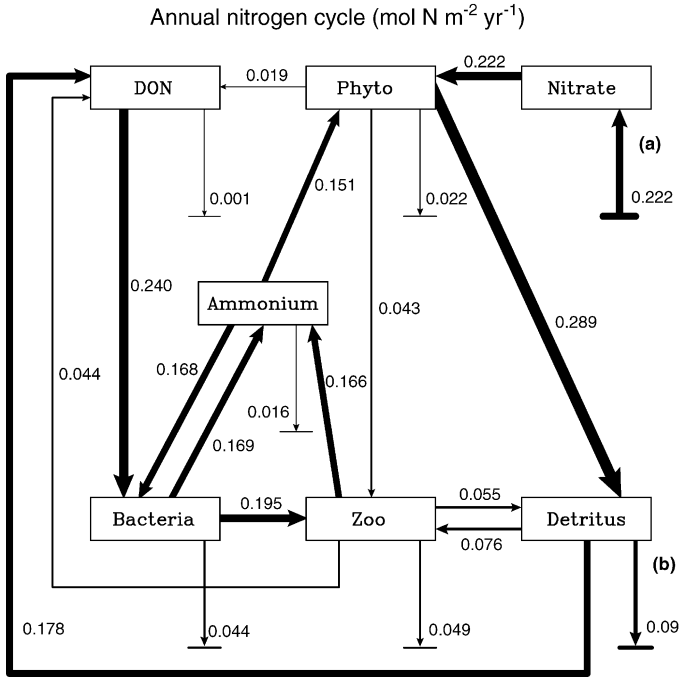

Fig. 7. Same as Fig. 6 but the parameters were estimated from assimilation of the BATS observations between 1988 and 1993.

(regeneration minus uptake) is plotted in Fig. 8) is two orders of magnitude smaller than the uptake of NH_4 by phytoplankton. While mesozooplankton grazing on phytoplankton is of the same order of magnitude as the nano/microzooplankton grazing, mesozooplankton do not seem to be a key player in NH_4 regeneration. Finally, Roman et al. (1995) showed that most of the carbon in the surface waters of the Sargasso Sea near Bermuda cycles through the bacteria and flagellates, which is the case in our simulation.

In order to assess the impact of the new microbial loop model on the fluxes, we used the parameter set estimated with data assimilation but the DON and NH_4 uptake by bacteria were modeled as in FDM. As we can see by comparing Figs. 8 and 9, the NH_4 regeneration is from different sources. Using the FDM uptake formulation, the main source of NH_4 is from nano/microzooplankton excretion. In our model simulation, the NH_4 source is split between bacteria regeneration and nano/microzooplankton excretion. It has been argued that microzooplankton are mainly responsible for NH_4 regeneration. However, there is evidence that bacteria can be key players in NH_4 regeneration in highly productive coastal regions (Tupas and Koike, 1991; Cotner and Gardner, 1993). In Gerlache Strait during the 1989 spring, Tupas et al. (1994) found that the bacteria regenerated NH_4 at 2–4 times the rate at which they assimilated it and that bacteria can regenerate 27–55% of the total recycled NH_4. Karl et al. (1996) concluded that at least one-half of the recycled NH_4 is due to nano- and microzooplankton. NH_4 regeneration by bacteria in oligotrophic environments is only speculative at present.

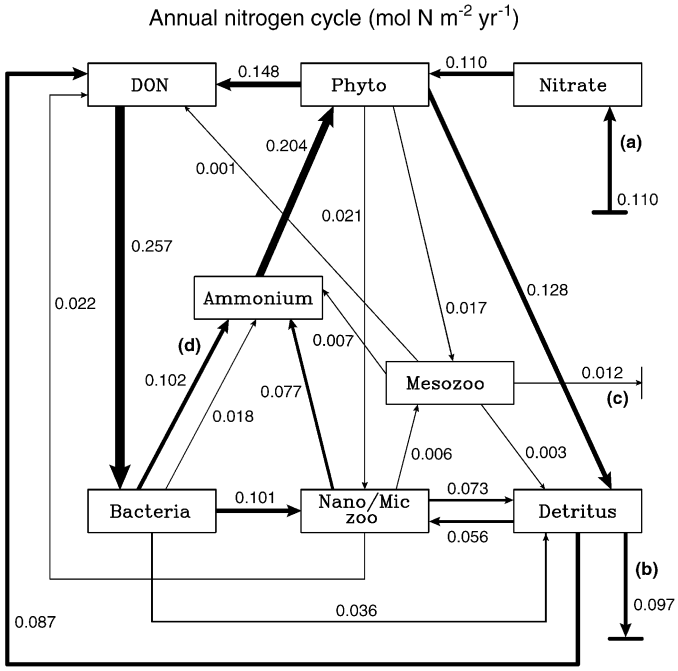

Fig. 8. Annual nitrogen cycle in mol N m^{-2} yr^{-1} obtained with the new model and parameters estimated from assimilation of the BATS observations between 1988 and 1993 (Table 1). (a) depicts the net nitrate upward flux (entrainment + diffusion), (b) the net detritus downward flux (volumetric dilution + sinking + diffusion), (c) the mortality by higher trophic levels, and (d) the NH_4 net regeneration by bacteria (regeneration − uptake).

6. Conclusions

This study represents an attempt to use data assimilation and observations from long-term time series to estimate not only the model parameters but also to guide the configuration of an ecosystem model for an oligotrophic environment. By assimilating the BATS observations, we were able to develop an ecosystem model with some degree of complexity, estimate the model parameters, and replicate the annual nitrogen cycle in the upper mixed layer.

Several modifications to the Fasham et al. (1990) model were found critical in the success of the BATS time series modeling. The adoption of a time varying chlorophyll to nitrogen ratio caused considerable improvement in the modeled chlorophyll *a* concentration. This is achieved by solving an equation for chlorophyll *a* according to the work of Geider et al. (1996). The most important modification that we adopted is the reformulation of the microbial loop. Our model of the microbial loop includes most of the processes described in the literature (e.g., Hellebust, 1974; Kirchman et al., 1989; Goldman and Dennett, 1991; Biddanda and Benner, 1997). We assume that the bacteria are energy limited rather than nutrient limited. The amount of available energy is in the form of DOC that is available. This DOC source is obtained from both the carbohydrate-DOM and the nitrogenous-DOM supply. The bacteria are allowed to: (a) take up and regenerate NH_4; (b) have a variable gross growth efficiency that changes with the C : N ratio of the DOM

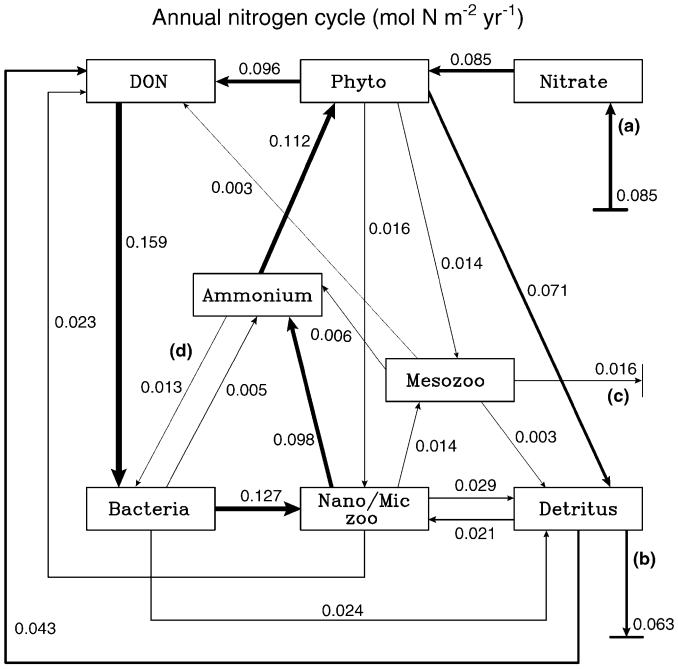

Fig. 9. Same as Fig. 8 but the model was run with a constant DON/NH_4 uptake by bacteria as defined in FDM. (d) represents only the NH_4 uptake by bacteria.

substrate; and (c) alter the C:N ratio of the DOM pool by taking up the required C and N substrates as they become available. Combination of these modifications and changes in the formulation of the NO_3 entrainment into the mixed layer (see Appendix A) led to a reduction of the new production by about half. Consequently, the new production was smaller than the regenerated production, which should be the case in an oligotrophic environment.

Using data assimilation, we were able to determine which processes in the microbial loop were dominant at BATS. We found that the bacteria regenerate NH_4 in an amount slightly larger than the amount due to zooplankton respiration. We also found that the bacterial uptake of NH_4 is much smaller than the uptake of DON. The capability of bacteria to take up and mineralize DOM could play an important role in controlling the size and rate of recycling of the DOC and DON pools in the ocean. The annual bacterial uptake of NH_4 was much smaller than the phytoplankton uptake of NH_4, which indicates that while the bacteria do compete with phytoplankton for NH_4 they do not outcompete phytoplankton. These conclusions still remain to be verified with field observations. However, there is a growing amount of evidence that the microbial loop is a key player in the carbon/nitrogen cycle. The modeling community also has begun to acknowledge the need for a better understanding of the microbial loop and of the role that bacteria play in the ecosystem.

While long-term time series, such as the two US JGOFS time series, are necessary to understand the functioning of the ecosystem and lead the development of models that can be coupled to ocean

general circulation models, the acquisition of more specific data is required. In order to assess the validity of our microbial loop model, a full analysis of the DOC and DON pool, its content in terms of HMW versus LMW, and carbohydrate versus nitrogenous material is necessary. Measurements of rates also would prove helpful to realize the ultimate goal of the modeling community, i.e. development of a predictive model.

Finally, we view this modeling effort as a first step towards the development of a more mechanistic model that will be coupled to a large-scale circulation model. The present model will have to be tested against other long-term time series such as the Hawaii Ocean Time series (HOT) and Ocean Station P. It will certainly need to include a better conversion of nitrogen to carbon if it is to be used to understand the carbon cycle, the main goal of the US JGOFS program.

Acknowledgements

We thank the scientists and technicians from the US JGOFS Bermuda Atlantic Time-Series program. In particular many thanks go to Drs. Anthony F. Michaels and Anthony H. Knap for their help and effort in compiling the BATS data set. We thank Dr. J.C. Gilbert for supplying the code and documentation for the optimization subroutine, N1QN3. We thank Drs. D. Hansell, C. Carlson and D. Steinberg for providing the data that were not available through the website. We thank Dr. D. Siegel for providing the PAR data. We thank J. Bartlett for editing the manuscript and Dr. S.C. Doney and an anonymous reviewer for comments and suggestions. This research was supported by NASA EOS contract NAGW-4596.

Appendix A. Model equations

A time-dependent box model of the ecosystem in the upper ocean mixed layer is presented which is a system of coupled ordinary differential equations. The model constituents include: phytoplankton, chlorophyll, nano/microzooplankton, mesozooplankton, bacteria, nitrate, ammonium, detrital nitrogen, detrital carbon, dissolved organic nitrogen, and dissolved organic carbon. The model is a modified version of the Fasham et al. (1990) (FDM) ecosystem model. We present the equations for the mixed layer depth and for each of the model constituents below.

A.1. Mixed layer depth equation

The mixed layer depth (MLD) is prescribed in the model using monthly mean climatological estimates of the MLD obtained from FDM. A time series of the seasonal variation of the MLD is then calculated from this estimate as

$$h(t) = \frac{\mathrm{dMLD}}{\mathrm{d}t}. \tag{A.1}$$

As in FDM, the model assumes that the seasonal shallowing of the mixed layer does not affect the biological fields within the mixed layer either by concentration or dilution processes. Unlike the FDM model, the assumption is made that none of the constituents are capable of vertically

migrating through the water so as to avoid being left behind as the mixed layer shallows. Also, the parameterization of the dilution and mixing process is reconsidered. In the FDM model, dilution occurred in the mixed layer during entrainment by assuming that the concentration of the model constituents just below the mixed layer depth were all zero, except for nitrate (NO_3), which was set to a constant higher concentration. Because the BATS data set did not show any relationship with depth for any of the model constituents except NO_3, it is assumed that the concentration of all the model constituents just below the mixed layer, except NO_3, are equal to that in the mixed layer. At BATS, the NO_3 concentration just below the MLD is observed to increase as the mixed layer depth increases. This modification effectively shuts off the dilution/concentration process and the cross-thermocline mixing, m, processes for all model constituents, except NO_3.

A.2. Phytoplankton [P; mmol N m^{-3}] equation

The time rate of change equation for the phytoplankton is written as

$$\frac{dP}{dt} = JQP - (\ _1 + \ _2 JQ)P - \ _1 P - G_1 - G_4, \tag{A.2}$$

where J is the specific growth rate under nutrient replete conditions, Q is the sum of the multiple nutrient limitation terms, $_1$ and $_2$ are the biomass-specific and growth-specific exudation rates, $_1$ is the biomass-specific phytoplankton mortality rate, and G_1 (Eq. (A.15)) and G_4 (Eq. (A.19)) are the grazing pressure terms due to grazing by the nano/microzooplankton and mesozooplankton, respectively.

The rate of specific growth under nutrient-replete conditions is defined as

$$J = \frac{1}{\mathrm{MLD}} \int_0^{\mathrm{MLD}} \frac{V_p \ I}{(V_p^2 + \ ^2 \ ^2 I^2)} \, dz, \tag{A.3}$$

where V_p is the phytoplankton maximum growth rate, is the initial slope of the P versus I curve, and the submarine irradiance field I is modeled as

$$I(z) = I_0 \, e^{-(\quad \ ^{\mathrm{Chl}})}, \tag{A.4}$$

where k and k are the seawater and chlorophyll-specific light attenuation coefficients, and the phytoplankton chlorophyll a to carbon ratio is calculated as

$$= \frac{\mathrm{Chl}a}{\mathrm{P}R_{\mathrm{C:N}}}, \tag{A.5}$$

where $R_{\mathrm{C:N}}$ is the phytoplankton carbon to nitrogen conversion ratio (mg C:mmol N), equivalent to $\mathrm{C:N_P}$ 12.

The amount of incident PAR at the surface of the ocean is computed as

$$I_0 = 0.8S \ E_0 \cos(\ )0.43(1 - \ )C_{\mathrm{corr}} \tag{A.6}$$

where S is the solar constant (1353 W m^{-2}) (Brock, 1981), E_0 is the correction to the solar constant due to the ellipse of the Earth's orbit (Duffie and Beckman, 1980), is the solar zenith

angle in radians, 0.43 is the amount of the solar constant within the spectral range of PAR, is the sea surface albedo, typically 0.04 (Payne, 1972), and

$$C_{corr} = (1.0 - C_{1} + (C_{2}\sin(\text{salt})))(1.0 - C(C_{3} + (C_{4}\cos(\text{salt})))), \tag{A.7}$$

is a local cloud correction algorithm where salt is the solar altitude, C is the monthly mean cloud amount in tenths from the Comprehensive Ocean-Atmosphere Data Set (COADS). The coefficients $C_{1}, \ldots, C_{4}$ have been locally fitted to the Bishop and Rossow (1991) solar radiation data set (Moisan and Niiler, 1998). A comparison between the modeled PAR and the measured PAR at BATS (Siegel et al., 1995) is shown in Fig. 4.

The effect due to nutrient limitation is parameterized by the sum of two modified Michaelis–Menten equations:

$$Q = Q_1 + Q_2 \leqslant 1, \tag{A.8}$$

where

$$Q_1 = \frac{\frac{NO_3}{_1} e^{- \; NH_4}}{1 + \frac{NO_3}{_1} + \frac{NH_4}{_2}}, \tag{A.9}$$

and

$$Q_2 = \frac{\frac{NH_4}{_2}}{1 + \frac{NO_3}{_1} + \frac{NH_4}{_2}}, \tag{A.10}$$

where K_1 and K_2 are the half-saturation coefficients for NO_3 and ammonium (NH_4), respectively. The term $\exp(- \; NH_4)$ is used to parameterize the effect of inhibition by NH_4 on the NO_3 uptake. The novelty of this modification is that it assures that the nutrient limitation term can only suppress the rate of phytoplankton growth ($Q \leqslant 1$). This term is a slightly modified version of the substitutive model of O'Neill et al. (1989) with the addition of the NO_3 uptake inhibition by NH_4, and is a merger of the FDM and the O'Neill et al. (1989) nutrient limitation models.

A.3. Chlorophyll a [Chla; mg chlorophyll a m^{-3}] equation

The phytoplankton component in the model is allowed to have a time-varying chlorophyll *a*-to-carbon ratio. The time rate of change equation for the phytoplankton chlorophyll pool is written as

$$\frac{d\text{Chl}a}{dt} = JQP_{\;\text{Chl}}\,\text{C:N}_\text{P}\text{MW}_\text{C} - {}_{1}\text{Chl}a - (G_1 + G_4)\frac{\text{Chl}a}{\text{P}}, \tag{A.11}$$

where $_{\text{Chl}}$ is the fraction of nitrogen assimilated by the phytoplankton that is used to make more chlorophyll, C:N_P, and MW_C are conversion constants and are presented in Table 1. The phytoplankton were assumed to not exude chlorophyll *a*.

The parameter $_{\text{Chl}}$ is calculated based upon Geider et al., (1996) and is written as

$$_{\text{Chl}} = \frac{QJ}{\text{PAR},} \tag{A.12}$$

where

$$\overline{\mathrm{PAR}} = \frac{1}{\mathrm{MLD}} \int_0^{\mathrm{MLD}} I_0 \mathrm{e}^{(\quad \mathrm{Chl})}\, \mathrm{d}z, \tag{A.13}$$

and and are the maximum and actual chlorophyll *a* to carbon ratios, respectively.

A.4. Nano/microzooplankton [Z; mmol N m^{-3}] equation

The model includes a nano/microzooplankton component that grazes on the phytoplankton, bacteria and detritus pools. The time rate of change of the nano/microzooplankton pool is written as

$$\frac{\mathrm{dZ}}{\mathrm{d}t} = (\ {}_1G_1 + \ {}_2G_2 + \ {}_3G_3)(1 - \ ) - \ {}_2\mathrm{Z} - G_5, \tag{A.14}$$

where ${}_1$, ${}_2$, and ${}_3$ are the assimilation efficiencies of the different food types, and G_1, G_2, and G_3 are the individual grazing rates upon phytoplankton (P), bacteria (B) and detrital nitrogen (DETN), respectively, and are written as

$$G_1 = g\,\mathrm{Z}\,\mathrm{P}\,\frac{\mathrm{P}}{K_3(\mathrm{P} + p_1\mathrm{B} + p_2\,\mathrm{DETN}) + \mathrm{P}^2 + p_1\mathrm{B}^2 + p_2\,\mathrm{DETN}^2} \tag{A.15}$$

$$G_2 = g\,\mathrm{Z}\,\mathrm{B}\,\frac{p_1\mathrm{B}}{K_3(\mathrm{P} + p_1\mathrm{B} + p_2\,\mathrm{DETN}) + \mathrm{P}^2 + p_1\mathrm{B}^2 + p_2\,\mathrm{DETN}^2} \tag{A.16}$$

$$G_3 = g\,\mathrm{Z}\,\mathrm{DETN}\,\frac{p_2\,\mathrm{DETN}}{K_3(\mathrm{P} + p_1\mathrm{B} + p_2\,\mathrm{DETN}) + \mathrm{P}^2 + p_1\mathrm{B}^2 + p_2\,\mathrm{DETN}^2}, \tag{A.17}$$

where g is the maximum biomass-specific grazing rate, K_3 is the half-saturation constant for ingestion, and p_1 and p_2 are the preferences for bacteria and detritus relative to phytoplankton. A growth-specific respiration term is included as . The mortality and excretion rates have been combined into a single biomass-specific term ${}_2$. This was done because the results from a previous data assimilation study (Spitz et al., 1998) demonstrated that the two terms were not independent of each other. One fraction of this loss term, , moves into the $\mathrm{NH_4}$ pool, another fraction, , moves into the dissolved organic nitrogen pool (DON), and the remainder (1 − −) is added to the detrital pool. G_5 (Eq. (A.20)) is the grazing pressure due to mesozooplankton.

A.5. Mesozooplankton [MZ; mmol N m^{-3}] equation

The model includes a mesozooplankton component that grazes on the phytoplankton and nano/microzooplankton pools. The time rate of change of the mesozooplankton pool is written as

$$\frac{\mathrm{dMZ}}{\mathrm{d}t} = (\ {}_4G_4 + \ {}_5G_5)(1 - \ {}_{\mathrm{gl}}) - \quad \mathrm{MZ}, \tag{A.18}$$

where ${}_4$ and ${}_5$ are the assimilation efficiencies of the different food types, and G_4 and G_5 are the individual grazing rates for phytoplankton (P) and nano/microzooplankton (Z) respectively, and

are written as

$$G_4 = g_1 MZ\,P \frac{P}{K_5(P + p_3 Z) + P^2 + p_3 Z^2}, \tag{A.19}$$

$$G_5 = g_1 MZ\,Z \frac{p_3\,Z}{K_5(P + p_3\,Z) + P^2 + p_3\,Z^2}, \tag{A.20}$$

where g_1 is the maximum biomass-specific grazing rate, K_5 is the half-saturation constant for ingestion, and p_3 is the preference for nano/microzooplankton relative to phytoplankton. A growth-specific respiration term is included as $_{g1}$. The mortality and excretion rates have been combined into a single biomass-specific term , and the loss terms are treated similarly to that in the nano/microzooplankton equation with similar terms, and .

A.6. Bacteria [B; mmol N m^{-3}] equation

The time rate of change of the bacterial pool is expressed as

$$\frac{dB}{dt} = U_{DON} + U_{NH_4} - {}_3B - {}_7B - G_2, \tag{A.21}$$

where U_{DON} is the rate of uptake of DON, U_{NH_4} is the net rate of uptake and regeneration of NH_4 (can be negative), $_3$ and $_7$ are the biomass-specific respiration and mortality terms, and G_2 is the grazing pressure from the nano/microzooplankton (Z). A derivation of the U_{DON} and U_{NH_4} terms is presented in Appendix B.

A.7. Nitrate [NO_3; mmol N m^{-3}] equation

The concentration of nitrate in the model changes over time as

$$\frac{dNO_3}{dt} = -JQ_1\,P + \frac{m + h\ (t)}{MLD}(N_{bottom} - NO_3), \tag{A.22}$$

where the first term is the total amount of NO_3 taken up by the phytoplankton, and the second term controls the amount injected or entrained from below the mixed layer. The second term combines the effects of diffusive mixing between the mixed layer and the deep ocean (m) and the concentration/dilution due to the deepening of the mixed layer ($h\ (t)$). Because only periods of mixed layer deepening are assumed to affect the model constituents, a mixed layer deepening term is defined as

$$h\ (t) = \max(h(t), 0). \tag{A.23}$$

Unlike FDM, we assume that the NO_3 concentration just below the mixed layer, N_{bottom}, is a function of depth and written as

$$N_{bottom} = \begin{cases} N_0 + ((MLD - 100)N_{slope}) & MLD > 100\ m \\ N_0 & MLD \leqslant 100\ m. \end{cases} \tag{A.24}$$

The depth of 100 m is chosen based on the NO_3 profiles at BATS and corresponds to the depth where the NO_3 concentration slope changes.

A.8. Ammonium [NH_4; mmol N m^{-3}] equation

The change in the concentration of ammonium with time is written as

$$\frac{\mathrm{dNH_4}}{\mathrm{d}t} = -JQ_2\mathrm{P} - U_{\mathrm{NH_4}} + \quad (\ {}_1G_1 + \ {}_2G_2 + \ {}_3G_3) + \ {}_{\mathrm{gl}}(\ {}_4G_4 + \ {}_5G_5) + \ {}_3\mathrm{B} + \ {}_2\mathrm{Z} + \quad \mathrm{MZ}, \tag{A.25}$$

where the first term is the uptake of NH_4 by the phytoplankton, the second term is the net uptake/regeneration of NH_4. The derivation for this latter term is presented in detail in Appendix B. The third and fourth terms represent the growth-specific respiration from the nanomicrozooplankton and mesozooplankton, respectively. The final three terms represent the biomass-specific respiration processes of the bacteria, nanomicrozooplankton and mesozooplankton, respectively.

A.9. Detrital nitrogen [DETN; mmol N m^{-3}] equation

The change in the concentration of detrital nitrogen with time is written as

$$\frac{\mathrm{dDETN}}{\mathrm{d}t} = (1 - \ {}_1)G_1 + (1 - \ {}_2)G_2 - \ {}_3G_3 - (\ {}_4 + \ {}_6\mathrm{B})\mathrm{DETN} + \ {}_1\mathrm{P} + \ {}_7\mathrm{B} + (1 - \ - \ )\ {}_2\mathrm{Z} + (1 - \ - \ )\ \mathrm{MZ} - \frac{V}{\mathrm{MLD}}\mathrm{DETN}, \tag{A.26}$$

where the first two terms account for the egestion processes of the nanomicrozooplankton, the third term is the net uptake of detritus by the nanomicrozooplankton (ingestion-egestion), and the fourth term is the rate of detrital breakdown to the dissolved organic pool, due to both dissolution and bacteria-mediated processes. The fifth and sixth terms are phytoplankton and bacteria mortality rates. The seventh term is the flux of nanomicrozooplankton mortality to the detrital pool. The final term accounts for the sinking of detritus out through the bottom of the mixed layer at a rate V. Fecall pellets from mesozooplankton are considered heavy enough to fall directly out of the mixed layer.

A.10. Detrital carbon [DETC; mmol C m^{-3}] equation

The change in the concentration of detrital carbon with time is written as

$$\frac{\mathrm{dDETC}}{\mathrm{d}t} = (1 - \ {}_1)G_1\mathrm{C{:}N_P} + (1 - \ {}_2)G_2\mathrm{C{:}N_B} - \ {}_3G_3\frac{\mathrm{DETC}}{\mathrm{DETN}} - (\ {}_4 + \ {}_6\mathrm{B})\mathrm{DETC} + \ {}_1\mathrm{PC{:}N_P} + \ {}_7\mathrm{BC{:}N_B}$$

$$+(1- \quad - \ )\ {}_2\mathrm{ZC:N_Z} + (1- \quad - \ )\quad \mathrm{MZC:N_Z}$$

$$-\frac{V}{\mathrm{MLD}}\mathrm{DETC}, \tag{A.27}$$

where all of the terms are similar to those in the DETN equation except that the changes in the C:N ratios have been accounted for.

A.11. Dissolved organic nitrogen [DON; mmol N m^{-3}] equation

The change in the concentration of dissolved organic nitrogen with time is written as

$$\frac{\mathrm{dDON}}{\mathrm{d}t} = (\ {}_4 + \ {}_6\mathrm{B})\mathrm{DETN} + \quad {}_2\mathrm{Z} + \quad \mathrm{MZ}$$

$$+(\ {}_1 + \ {}_2JQ)\mathrm{P} - U_{\mathrm{DON}}, \tag{A.28}$$

where the first term is the flux of nitrogen from the detrital pool, the second and third terms represent the flux of respiration and mortality from the nanomicrozooplankton and mesozooplankton, respectively, the fourth term is the flux of nitrogen from the phytoplankton due to biomass- and growth-specific exudation, and the final term is the rate of uptake of DON by bacteria.

A.12. Dissolved organic carbon [DOC; mmol C m^{-3}] equation

The change in the concentration of dissolved organic carbon with time is written as

$$\frac{\mathrm{dDOC}}{\mathrm{d}t} = (\ {}_4 + \ {}_6\mathrm{B})\mathrm{DETC} + \quad {}_2\mathrm{ZC:N_Z} + \quad \mathrm{MZC:N_Z}$$

$$+(\ {}_1 + \ {}_2JQ)\mathrm{PC:N_P} + P \quad - U_{\mathrm{DOC}}, \tag{A.29}$$

where most of the terms are similar to those in the DON equation except that the changes in the C:N ratios have been accounted for. Phytoplankton also are allowed to excrete excess DOC during periods when the amount of energy being harvested is greater than that required for growth under the nutrient conditions present.

$$P = \begin{cases} {}_3(\text{—}_{\mathrm{p}} - Q)J\mathrm{PC:N_P} & J/V_{\mathrm{p}} > Q, \\ 0 & J/V_{\mathrm{p}} \leqslant Q. \end{cases} \tag{A.30}$$

Appendix B. Bacterial uptake terms

The first assumption made is that the bio-active fraction of the dissolved organic matter is composed primarily of a carbohydrate and a nitrogenous pool. Accordingly, the DON pool is composed completely of the nitrogenous material, $\mathrm{DON_{nitro}}$, which is assumed to have a constant C:N ratio ($\mathrm{C:N_{DON}}$) that reflects the mean composition of the pool. The DOC pool is composed of

both nitrogenous and carbohydrate fractions, DOC_{nitro} and DOC_{carbo}, respectively, such that

$$DOC_{total} = DOC = DOC_{carbo} + DOC_{nitro}. \tag{B.1}$$

The amount of DOC within the nitrogenous pool is calculated as

$$DOC_{nitro} = DON\, C{:}N_{DON}, \tag{B.2}$$

with the remaining fraction in the DOC pool going into the carbohydrate fraction as

$$DOC_{carbo} = DOC - DON\, C{:}N_{DON}. \tag{B.3}$$

The total amount of nitrogen taken up by the bacteria for growth is written as

$$U = U_{DON} + U_{NH_4}, \tag{B.4}$$

where U_{DON} is equal to the amount of DON taken up by the bacteria, and U_{NH_4} is the net amount of NH_4 taken up or released by the bacteria. The maximum amount of nitrogen that the bacteria are allowed to take up is written as

$$U_{max} = V_b B, \tag{B.5}$$

where V_b is the maximum biomass-specific rate of nitrogen uptake. By assuming that bacteria prefer to take up DON over NH_4, the amount of DON that the bacteria can take up can be written as

$$U_{DON} = V_b B \frac{DON}{K_{nitro} + DON}, \tag{B.6}$$

where K_{nitro} is the half-saturation coefficient for DON uptake. After accounting for the gross growth efficiency of nitrogenous DOM, GGE_{nitro}, and using the nitrogenous DOM for balanced growth of the bacteria, the amount of excess nitrogen that can be further used with the carbohydrate pool for growth or regenerated as NH_4 is written as

$$U_{nitro} = V_b B \frac{DON}{K_{nitro} + DON}\left(1 - \frac{C{:}N_{DON}\, GGE_{nitro}}{C{:}N_B}\right). \tag{B.7}$$

The maximum rate at which NH_4 is taken up by the bacteria is calculated as the difference between the maximum rate of nitrogen uptake and the DON uptake, $V_b B - U_{DON}$. The actual rate at which NH_4 is taken up is controlled by the availability of both NH_4 and carbohydrate DOM and can be written as

$$U_{ammon} = (V_b B - U_{DON}) \frac{NH_4}{K_{NH_4} + NH_4} \frac{DOC_{carbo}}{K_{carbo} + DOC_{carbo}}, \tag{B.8}$$

where K_{carbo} and K_{NH_4} are the half-saturation coefficients for the carbohydrate DOM and NH_4, respectively.

The uptake of carbohydrate DOM is written as

$$U_{carbo} = \frac{DOC_{carbo}}{K_{carbo} + DOC_{carbo}} U_{nitro} + U_{ammon} \frac{C{:}N_B}{GGE_{carbo}}, \tag{B.9}$$

where GGE_{carbo} is the bacteria gross growth efficiency of carbohydrate DOM.

Finally, the amount of NH_4 regenerated by the bacteria through uptake of the nitrogenous DOM is written as

$$U_{\text{regen}} = U_{\text{nitro}} \left(1 - \frac{\text{DOC}_{\text{carbo}}}{K_{\text{carbo}} + \text{DOC}_{\text{carbo}}}\right). \tag{B.10}$$

Using the above definitions, the amount of DOC taken up by the bacteria is written as

$$U_{\text{DOC}} = U_{\text{carbo}} + U_{\text{DON}}\,\text{C}:\text{N}_{\text{DON}}. \tag{B.11}$$

And, the net uptake or release (uptake-regeneration) of NH_4 is written as

$$U_{\text{NH}_4} = U_{\text{ammon}} - U_{\text{regen}}. \tag{B.12}$$

Appendix C. Root-mean square error and correlation

To evaluate qualitatively the performance of the data assimilation, two quantities were computed: the root-mean-square (rms) error defined as

$$\text{rms} = \left(\frac{1}{N}\sum_{=1}(a - d)^2\right)^{1/2}, \tag{C.1}$$

and the correlation coefficient (r) given by

$$r = \frac{\sum_{=1}(a - a)(d - d)}{\left(\sum_{=1}(a - a)^2 \sum_{=1}(d - d)^2\right)^{1/2}} \tag{C.2}$$

where d and a are the data and model equivalents to the data, respectively, and the "over bar" denotes time mean values. N is equal to the number of observations for the five year (1988–1993) assimilation window. Each year, the monthly cruises take place at different dates. Corresponding model results from the same dates are used for the comparison.

The root-mean-square error is a measure of the difference between model results and observations while the correlation coefficient gives a measure of the phase shift. It is important to consider all quantities when evaluating the success of the data assimilation. Indeed, a small root-mean-square error with a small correlation indicates a phase shift between the observations and the model results, an indication of poor performance of the data assimilation procedure.

References

Anderson, T.R., 1992. Modeling the influence of food C:N ratio, and respiration on growth and nitrogen excretion in marine zooplankton and bacteria. Journal of Plankton Research 14, 1645–1671.

Armstrong, R.A., Sarmiento, J.L., Slater, R.D., 1995. Monitoring ocean productivity by assimilating satellite chlorophyll into ecosystem models. In: Powell, T.M., Steele, J.H. (Eds.), Ecological Time Series. Chapmann & Hall, London, pp. 371–390.

Baines, S.B., Pace, M.L., 1991. The production of dissolved organic matter by phytoplankton and its importance to bacteria: patterns across marine and freshwater systems. Limnology and Oceanography 36, 1078–1090.

Biddanda, B., Benner, R., 1997. Carbon, nitrogen, and carbohydrate fluxes during the production of particulate and dissolved organic matter by marine phytoplankton. Limnology and Oceanography 42, 506–518.

Bishop, J.K.B., Rossow, W.B., 1991. Spatial and temporal variability of global surface solar irradiance. Journal of Geophysical Research 96, 16 839–16 858.

Bissett, W.P., Walsh, J.J., Dieterle, D.A., Carder, K.L., 1999. Carbon cycling in the upper waters of the Sargasso Sea: I. Numerical simulation of differential carbon and nitrogen fluxes. Deep-Sea Research Part I 46, 205–269.

Bratbak, G., Thingstad, T.F., 1985. Phytoplankton-bacteria interactions: an apparent paradox? Analysis of a model system with both competition and commensalism. Marine Ecology Progress Series 25, 23–30.

Brock, T.D., 1981. Calculating solar radiation for ecological studies. Ecological Modelling 14, 1–19.

Campbell, L., Vaulot, D., 1993. Photosynthetic picoplankton community structure in the subtropical North Pacific Ocean near Hawaii (station ALOHA). Deep-Sea Research II 40, 2043–2060.

Carlson, C.A., Ducklow, H.W., 1995. Dissolved organic carbon in the upper ocean of the central Equatorial Pacific, 1992: daily and fine scale vertical variations. Deep-Sea Research I 42, 639–656.

Carlson, C.A., Ducklow, H.W., 1996. Growth of bacterioplankton and consumption of dissolved organic carbon in the Sargasso Sea. Aquatic Microbial Ecology 10, 69–85.

Carlson, C.A., Ducklow, H.W., Sleeter, Th.D., 1996. Stocks and dynamics of bacterioplankton in the northwestern Sargasso Sea. Deep-Sea Research II 43, 491–515.

Carlson, D.J., Brann, M.L., Mague, T.H., Mayer, L.M., 1985. Molecular weight distribution of dissolved organic matter in seawater determined by ultrafiltration: a reexamination. Marine Chemistry 16, 155–171.

Caron, D.A., Dam, H.G., Kremer, P., Lessard, E.J., Madin, L.P., Malone, T.C., Napp, J.M., Peele, E.R., Roman, M.R., Youngbluth, M.J., 1995. The contribution of microorganisms to particulate carbon and nitrogen in surface waters of the Sargasso Sea near Bermuda. Deep-Sea Research I 42, 943–972.

Cloern, J.E., Grenz, C., Vidergar-Lucas, L., 1995. An empirical model of the phytoplankton chlorophyll:carbon ratio – the conversion between productivity and growth. Limnology and Oceanography 7, 1310–1313.

Cotner Jr., J.B., Gardner, W.S., 1993. Heterotrophic bacterial mediation of ammonium and dissolved free amino acid fluxes in the Mississippi River plume. Marine Ecological Progress Series 93, 75–87.

Currie, D.L., Kalff, J., 1984a. A comparison of the abilities of freshwater algae and bacteria to acquire and retain phosphorus. Limnology and Oceanography 29, 298–310.

Currie, D.L., Kalff, J., 1984b. Can bacteria outcompete phytoplankton for phosphorous? A chemostat test. Microbial Ecology 10, 205–216.

Doney, S.C., 1996. A synoptic atmospheric surface forcing data set and physical upper ocean model for the US JGOFS Bermuda Atlantic Time-Series (BATS) site. Journal of Geophysical Research 101, 25 615–25 634.

Doney, S.C., Glover, D.M., Najjar, R.G., 1996. A new coupled, one-dimensional biological-physical model for the upper ocean: applications to the JGOFS Bermuda Atlantic Time-series Study (BATS) site. Deep-Sea Research II 43, 591–624.

Druffel, E.R.M., Williams, P.M., Bauer, J.E., Ertel, J.R., 1992. Cycling of dissolved and particulate organic matter in the open ocean. Journal of Geophysical Research 97, 15 639–15 659.

Duffie, J.A., Beckman, W.A., 1980. Solar Engineering of Thermal Processes. Wiley-Interscience, New York, NY, 762pp.

Eppley, R.W., 1972. Temperature and phytoplankton growth in the sea. Fishery Bulletin 90, 1063–1085.

Evans, G.T., Parslow, J.S., 1985. A model of annual plankton cycles. Biology and Oceanography 3, 327–347.

Fasham, M.J.R., Evans, G.T., 1995. The use of optimisation techniques to model marine ecosystem dynamics at the JGOFS station at 47°N 20°W. Philosophical Transactions of the Royal Society of London B348, 206–209.

Fasham, M.J.R., Ducklow, H.W., McKelvie, S.M., 1990. A nitrogen-based model of plankton dynamics in the oceanic mixed-layer. Journal of Marine Research 48, 591–639.

Fasham, M.J.R., Sarmiento, J.L., Slater, R.D., Ducklow, H.W., Williams, R., 1993. Ecosystem behavior at Bermuda Station "S" and Ocean Weather Station "India": a general circulation model and observational analysis. Global Biogeochemical Cycles 7, 379–415.

Fogg, G.E., 1983. The ecological significance of extracellular products of phytoplankton photosynthesis. Botanica Marina 26, 3–14.

Frost, B.W., 1987. Grazing control of phytoplankton stock in the subarctic Pacific: a model assessing the role of mesozooplankton, particularly the large calanoid copepods, Neocalanus spp. Marine Ecology Progress Series 39, 49–68.

Geider, R.J., 1987. Light and temperature dependence of the carbon to chlorophyll ratio in microalgae and cyanobacteria: implications for physiology and growth of phytoplankton. New Phytology 106, 1–34.

Geider, R.J., 1993. Quantitative phytoplankton ecophysiology: implications for primary production and phytoplankton growth. ICES Marine Science Symposium 197, 52–62.

Geider, R.J., MacIntyre, H., Kana, T.M., 1996. A dynamic model of photoadaptation in phytoplankton. Limnology and Oceanography 41, 1–15.

Geider, R.J., MacIntyre, H., Kana, T.M., 1997. Dynamic model of phytoplankton growth and acclimation: responses of the balanced growth rate and the chlorophyll *a*: carbon ratio to light, nutrient-limitation and temperature. Marine Ecology Progress Series 148, 187–200.

Gilbert, J.-Ch., Lemaréchal, C., 1989. Some numerical experiments with variable-storage quasi-Newton algorithms. Mathematical Programming 45, 407–435.

Goldman, J.C., 1980. Physiological processes, nutrient availibility, and the concept of relative growth rate in marine phytoplankton ecology. In: Falkowski, P.G. (Ed.), Primary Productivity in the Sea. Plenum Press, New York, pp. 179–193.

Goldman, J.C., Dennett, M.R., 1991. Ammonium regeneration and carbon utilization by marine bacteria grown on mixed substrates. Marine Biology 109, 369–378.

Goldman, J.C., Caron, D.A., Dennett, M.R., 1987. Regulation of gross growth efficiency and ammonium regeneration in bacteria by substrate C:N ratio. Limnology and Oceanography 32, 1239–1252.

Hansen, P.J., Björnsen, P.K., Hansen, B.W., 1997. Zooplankton grazing and growth: Scaling within the 2-2,000- m body size range. Limnology and Oceanography 42, 687–704.

Harrison, W.G., Harris, L.R., Irwin, B.D., 1996. The kinetics of nitrogen utilization in the oceanic mixed layer: nitrate and ammonium interactions at nanomolar concentrations. Limnology and Oceanography 41, 16–32.

Hellebust, J.A., 1974. Extracellular products. Botanical Monographs 10, 838–863.

Hofmann, E.E., Lascara, C.M., 1998. Overview of interdisciplinary modeling for marine ecosystems. In: Robinson, A.R., Brink, K.H. (Eds.), The Sea, The Global Coastal Ocean: Processes and Methods, Vol. 10. Wiley, New York, pp. 507–540.

Hurtt, G.C., Armstrong, R.A., 1996. A pelagic ecosystem model calibrated with BATS data. Deep-Sea Research II 43, 653–683.

Jenkins, W.J., 1988. Nitrate flux into the euphotic zone near Bermuda. Nature 331, 521–523.

Jenkins, W.J., Goldman, J.C., 1985. Seasonal oxygen cycling and primary production in the Sargasso Sea. Journal of Marine Research 43, 465–491.

Kana, T.M., Gilbert, P.M., 1987. Effect of irradiance up to 2000 E m^{-2} s^{-1} on marine Synechococcus WH7803-I. Growth, pigmentation, and cell composition. Deep-Sea Research I 34, 479–495.

Karl, D.M., Christian, J.R., Dore, J.E., Letelier, R.M., 1996. Microbiological oceanography in the region west of the Antarctic Peninsula: microbial dynamics, nitrogen cycle and carbon flux. In: Foundations for Ecological Research West of the Antarctic Peninsula, Antarctic Research Series, Vol. 70, pp. 303–332.

Karl, D.M., Hebel, D.V., Björkman, K., Letelier, R.M., 1998. The role of dissolved organic matter exudation in the productivity of the oligotrophic North Pacific Ocean. Limnology and Oceanography 43, 1270–1286.

Kiefer, D.A., 1993. Modelling growth and light absorption in the marine diatom Skeletonema costatum. In: Evans, G.T., Fasham, M.J.R. (Eds.), Towards a Model of Ocean Biogeochemical Processes. Springer, Berlin, pp. 91–121.

Kirchman, D.L., Keil, R.G., Wheeler, P.A., 1989. The effect of amino acids on ammonium utilization and regeneration by heterotrophic bacteria in the subarctic Pacific. Deep-Sea Research I 36, 1763–1776.

Lancelot, C., Billen, G., 1985. Carbon-nitrogen relationships in nutrient metabolism of coastal marine ecosystems. In: Jannasch, H.W., Williams, P.J.LeB. (Eds.), Advances in Aquatic Microbiology, Vol. 3. Academic Press, New York, pp. 263–321.

Laws, E.A., Bannister, T.T., 1980. Nutrient- and light-limited growth of Thalassiosira fluvialtilis in continuous culture, with implications for phytoplankton growth in the ocean. Limnology and Oceanography 25, 457–473.

Lawson, L.M., Spitz, Y.H., Hofmann, E.E., Long, R.B., 1995. A data assimilation technique applied to a predator-prey model. Bulletin of Mathematical Biology 57, 593–617.

Lawson, L.M., Hofmann, E.E., Spitz, Y.H., 1996. Time series sampling and data assimilation in a simple marine ecosystem model. Deep-Sea Research II 43, 625–651.

Letelier, R.M., Bidigare, R.R., Hebel, D.V., Ondrusek, M., Winn, C.D., Karl, D.M., 1993. Temporal variability of phytoplankton community structure based on pigment analysis. Limnology and Oceanography 38, 1420–1437.

Levitus, 1982. Climatological atlas of the world. NOAA Professional Paper, 30.

Lipschultz, F., Zafiriou, O.C., Ball, L.A., 1996. Seasonal fluctuations of nitrite concentrations in the deep oligotrophic ocean. Deep-Sea Research II 43, 403–420.

Mague, T.H., Friberg, E., Hughes, D.J., Morris, I., 1980. Extracellular release of heterotrophic dinoflagellates in oceanic waters, measured with a dual-beam radioisotope technique. Marine Biology 87, 289–296.

Malone, T.C., Pike, S.E., Conley, D.J., 1993. Transient variations in phytoplankton productivity at the JGOFS Bermuda time series station. Deep-Sea Research I 40, 903–924.

Matear, R.J., 1995. Parameter optimization and analysis of ecosystem models using simulated annealing: a case study at Station P. Journal of Marine Research 53, 571–607.

McCarthy, M.M., Hedges, J.I., Benner, R., 1998. Major bacterial contribution to marine dissolved organic nitrogen. Science 281, 231–234.

McGillicuddy Jr., D.J., McCarthy, J.J., Robinson, A.R., 1995a. Coupled physical and biological modelling of the spring bloom in the North Atlantic (I): model formulation and one dimensional bloom processes. Deep-Sea Research I 42, 1313–1357.

McGillicuddy Jr., D.J., Robinson, A.R., McCarthy, J.J., 1995b. Coupled physical and biological modelling of the spring bloom in the North Atlantic (II): three dimensional bloom and post-bloom processes. Deep-Sea Research I 42, 1359–1398.

Menzel, D.W., Ryther, J.H., 1960. The annual cycle of primary production in the Sargasso Sea off Bermuda. Deep-Sea Research I 6, 351–367.

Michaels, A.F., Knap, A.H., 1996. Overview of the U.S. JGOFS Bermuda Atlantic Time-series Study and the Hydrostation S program. Deep-Sea Research II 43, 157–198.

Michaels, A.F. Knap, A.H. Dow, R.L., Gurdensen, K., Johnson, R.J., Sorenson, J., Close, A., Knauer, G.A., Lohrenz, S.E., Asper, V.A., Tuel, M., Bidigare, R.R., 1994. Seasonal patterns of ocean biogeochemistry at the U.S. JGOFS Bermuda Atlantic Time-series Study site. Deep-Sea Research I 41, 1013–1038.

Moisan, J.R., Niiler, P.P., 1998. The seasonal heat budget of the north Pacific: Net heat flux and heat storage rates (1950–1990). Journal of Physical Oceanography 28, 401–421.

Moisan, J.R., Hofmann, E.E., Haidvogel, D.B., 1996. Modeling nutrient and plankton processes in the California coastal transition zone. 2. A three-dimensional physical-bio-optical model. Journal of Geophysical Research 101, 22 677–22 691.

Oguz, T., Ducklow, H., Malanotte-Rizzoli, P., Tugrul, S., Nezlin, N.P., Unluata, U., 1996. Simulation of annual plankton productivity cycle in the Black Sea by a one-dimensional physical-biological model. Journal of Geophysical Research 101, 16 585–16 599.

O'Neill, R.V., Angelis, D.L., Pastor, J.J., Jackson, B.J., Post, W.M., 1989. Multiple nutrient limitation in ecological models. Ecological Modeling 46, 147–163.

Parker, R.R., Sibert, J., Brown, T.J., 1975. Inhibition of primary production through heterotrophic competition for nitrate in a stratified estuary. Journal of the Fisheries Research Board of Canada 32, 72–77.

Parsons, T.R., Albright, L.J., Whitney, F., Wong, C.S., Williams, P.J., 1981. The effect of glucose on the productivity of seawater: an experimental approach using controlled aquatic ecosystems. Marine Environment Research 4, 229–242.

Payne, R.E., 1972. Albedo of the sea surface. Journal of Atmospheric Sciences 29, 959–970.

Platt, T., Harrison, W.G., 1985. Biogenic fluxes of carbon and oxygen in the ocean. Nature 318, 55–58.

Prunet, P., Minster, J.-F., Ruiz-Pino, D., Dadou, I., 1996a. Assimilation of surface data in one-dimensional physical-biogeochemical model of the surface ocean: 1. Method and preliminary results. Global Biogeochemical Cycles 10, 111–138.

Prunet, P., Minster, J.-F., Echevin, V., Dadou, I., 1996b. Assimilation of surface data in one-dimensional physical-biogeochemical model of the surface ocean: 2. Adjusting a simple trophic model to chlorophyll, temperature, nitrate, and pCO_2 data. Global Biogeochemical Cycles 10, 139–158.

Rhee, G.-Yull, 1972. Competition between an alga and an aquatic bacterium for phosphate. Limnology and Oceanography 17, 505–514.

Roman, M.R., Dam, H.G., Gauzens, A.L., Napp, J.M., 1993. Zooplankton biomass and grazing at the JGOFS Sargasso Sea time series station. Deep-Sea Research I 40, 883–901.

Roman, M.R., Caron, D.A., Kremer, P., Lessard, E.J., Madin, L.P., Malone, T.C., Napp, J.M., Peele, E.R., Youngbluth, M.J., 1995. Spatial and temporal changes in the partioning of organic carbon in the plankton community of the Sargasso Sea off Bermuda. Deep-Sea Research I 42, 973–992.

Santschi, P.H., Guo, L., Baskaran, M., Trumbore, S., Southon, J., Bianchi, T.S., Honeyman, B., Cifuentes, L., 1995. Isotopic evidence for the contemporary origin of high-molecular weight organic matter in oceanic environments. Geochimica et Cosmochimica Acta 59, 625–631.

Sarmiento, J.L., Slater, R.D., Fasham, M.J.R., Ducklow, H.W., Toggweiler, J.R., Evans, G.T., 1993. A seasonal three-dimensional ecosystem model of nitrogen cycling in the north Atlantic euphotic zone. Global Biogeochemical Cycles 7, 417–450.

Scientific Committee on Oceanic Research (SCOR), 1990. The Joint Global Ocean Flux Study (JGOFS) science plan. JGOFS Report No. 5. International Council of Scientific Unions, 61 pp.

Siegel, D.A., Michaels, A.F., Sorensen, J.C., O'Brien, M.C., Hammer, M.A., 1995. Seasonal variability of light availability and utilization in the Sargasso Sea. Journal of Geophysical Research 100, 8695–8713.

Sieracki, M.E., Haugen, E.M., Cucci, T.L., 1995. Overestimation of heterotrophic bacteria in the Sargasso Sea: direct evidence by flow and imaging cytometry. Deep-Sea Research I 42, 1399–1409.

Spitz, Y.H., Moisan, J.R., Abbott, M.R., Richman, J.G., 1998. Data assimilation and a pelagic ecosystem model: parameterization using time series observations. Journal of Marine Systems 16, 51–68.

Spitzer, W.S., Jenkins, W.J., 1989. Rates of vertical mixing, gas exchange and new production: estimates from seasonal gas cycles in the upper ocean near Bermuda. Journal of Marine Research 47, 169–196.

Steele, J.H., Henderson, E.W., 1992. The role of predation in plankton models. Journal of Plankton Research 14, 157–172.

Tupas, L., Koike, I., 1991. Simultaneous uptake and regeneration of ammonium by mixed assemblages of heterotrophic marine bacteria. Marine Ecology Progress Series 70, 273–282.

Tupas, L.M., Koike, I., Karl, D.M., Holm-Hansen, O., 1994. Nitrogen metabolism by heterotrophic bacterial assemblages in Antarctic coastal waters. Polar Biology 14, 195–204.

Vallino, J.J., Hopkinson, C.S., Hobbie, J.E., 1996. Modeling bacterial utilization of dissolved organic matter: optimization replaces Monod growth kinetics. Limnology and Oceanography 41, 1591–1609.

Walsh, J.J., Dugdale, R.C., 1972. Nutrient submodels and simulation models of phytoplankton production in the sea. In: Kramer, J., Allen, H. (Eds.), Nutrients in Natural Waters. Wiley, New York, pp. 171–191.

Wheeler, P.A., Kokkinakis, S.A., 1990. Ammonium recycling limits nitrate use in the oceanic subarctic Pacific. Limnology and Oceanography 35, 1267–1278.

Williams, P.J. LeB., 1984. Bacterial production in the marine food chain: the emperor's new suit of clothes? In: Fasham, M.J.R. (Ed.), Flows of Energy and Materials in Marine Ecosystems, Theory and Practice. Plenum Press, New York, pp. 271–299.

Williams, P.J. Le B., 1990. The importance and losses during microbial growth: commentary on the physiology, measurement and ecology of the release of dissolved organic material. Marine Microbial Food Webs 4 (2), 175–206.

Wroblewski, J.S., 1977. A model of phytoplankton plume formation during variable upwelling. Journal of Marine Research 35, 357–394.